NUCLEONIC LUNAR RANGING AND
TRACKING SYSTEM

FINAL REPORT

ER-416

$N68$ 23553

Prepared for

National Aeronautics and Space Administration
George C. Marshall Space Flight Center
Huntsville, Alabama   35812

In Support of

Contract   NAS8-20562

Prepared by:

GENERAL NUCLEONICS DIVISION
Tyco Laboratories, Inc.
115 South Spring Street
Claremont, California 91711

TABLE OF CONTENTS

TABLE OF CONTENTS
(Continued)

LIST OF ILLUSTRATIONS

TABLE OF CONTENTS
(Continued)

1.0   INTRODUCTION

This report summarizes the analyses, development, design, fabrication and feasibility test demonstration of a Nucleonic Lunar Ranging and Tracking System. This work was accomplished under Contract NAS8-20562 for NASA, George C. Marshall Space Flight Center, Huntsville, Alabama. The purpose of the contract was to determine the best type of nuclear radiation available to measure the altitude and altitude rate of a lunar landing vehicle as it approaches the lunar surface, and then determine whether such a device is indeed feasible and whether it has definite advantages over existing types of altimeters.

The reason for investigating the nucleonic approach was because this highly penetrating radiation is not affected significantly by the ionized rocket exhaust, and its capability for high accuracy at low altitudes. All of the practical types of nuclear radiation were considered for this application. These included neutrons, high energy particles, and photon radiation in the form of x-rays and gamma rays. The types of radiation sources were both natural, coming from isotope sources, and machine generated, coming from x-ray tubes, neutron guns or particle guns. A careful tradeoff study determined that a pulse x-ray time-of-flight measurement technique was the optimum.

The pulse time-of-flight measuring technique involves first generating an extremely short burst of x-rays and measuring the time taken for the x-rays, traveling at the speed of light, to travel

1.0 INTRODUCTION (Continued)

the distance to the lunar surface and return to the landing vehicle. Penetrating x-ray radiation allows the equipment to be located inside the vehicle skin since it can easily penetrate the wall of the landing vehicle. Frequency of the high energy photons is so high that it does not interact with the molecular or atomic structure of the ionized gases but rather with the electrons themselves. Therefore, no increased absorption is caused by the fact that the gases are ionized as is the case with lower frequency microwave radiation. By measuring the time of flight rather than the magnitude of returning radiation, as used in several techniques, the system is independent of the amount of gas absorption or change in sensitivity of components in either the source or the detector unit.

Three areas involved with this approach required designs pushing the state-of-the-art in ruggedized hardware and design: 1) the x-ray unit, 2) the packaging of extremely high voltages within very small volume, and 3) extremely fast electronics for both measurement of extremely short periods and also generating of extremely fast pulses. Much of the hardware and designs required for this advanced concept were developed by General Nucleonics personnel in a previous classified contract for ballistic reentry vehicles. The x-ray tube selected was developed on this previous contract, and is the ML-645 x-ray tube manufactured by Machlett Labs. It is capable of plate voltages up to 125,000 volts, peak plate currents of 20 amperes, pulse widths of 15 nanoseconds, and

1.0 INTRODUCTION (Continued)

besides these extreme characteristics, the tube is ruggedized to withstand 100 g environment. This tube has an envelope of only 5 inches long by 2 inches in diameter and weighs only 0.8 pounds. Driving the x-ray tube is a grid drive modulator. The grid drive modulator is composed of a modulator oscillator which in turn drives the grid drive pulser with a 400 volt 15 nanosecond pulse. The x-ray tube voltage is supplied by a Cockcroft Walton multiplier type power supply. An input voltage of 28 volts is first regulated and then converted to an AC signal which is fed to transformer and then multiplied up to 100,000 volts impressed across the x-ray tube. The x-rays are generated only when a grid drive pulse is applied to the grid of the x-ray tube.

Data processing electronics is made of a pulse time to amplitude converter, a storage unit and a buffer circuit which has an analog output of 0 to 5 volts linearly related to the altitude above the lunar surface. Signal is also fed through a differentiating circuit to obtain the rate of descent. This signal is also sent through a buffer circuit which readies it for display, telemetry, or control functions.   The time to voltage converter references both the x-ray tube pulse generation time and the return time of the x-ray pulse to the detector. Logic circuitry is used such that altitude measurement information is transferred to the storage only when proper detector pulse appears. The use of integrated circuits in the design of the electronics has resulted in an extremely small packaging capability.

1.0 INTRODUCTION (Continued)

The system was developed to operate in lunar atmosphere, where air backscatter and air attenuation of radiation is minimized. In order to simulate such a condition, the system was tested in the 60 foot diameter altitude chamber at NASA, Langley Research Center, Hampton, Virginia. The altitudes from touchdown to forty five feet could be simulated in this facility.

As a result of this program, it was determined that the Nucleonic Lunar Ranging and Tracking System has definite advantages over the more conventional microwave or radar altimeters. Among these advantages are: it is not affected by rocket exhaust and has increased accuracy especially at low altitude. This increased accuracy is primarily a result of the fact that the x-rays have no multiple bounce, that you receive direct path radiation which results in a well defined pulse shape. The breadboard hardware is packaged into a volume of 1,635 cubic inches with a weight of only 31.6 pounds. Reduction in size and weight is definitely feasible for flyable prototype units.

2.0 SYSTEMS DESIGN APPROACH

Three approaches to the NLRTS were considered:

1. Low Energy γ-Rays

2. Pulsed Isotope Approach

3. Pulsed X-Ray Tube

A brief description of the three approaches is given along with a tradeoff summary which shows the advantages of the Pulsed X-Ray Tube approach.

2.1 Low Energy γ-Rays

Range to the lunar surface and vertical velocity can be determined by emitting gamma photons and measuring the amount scattered from the lunar surface. In this case the detector must be shielded from the source since the emitted intensity is orders-of-magnitude larger than the backscattered flux and no practical means of discriminating between the emitted and scattered photons exist. A low energy γ emitter such as Am-241 would be used. A source strength of 100 to 1000 curies would be required. Low energy source strengths of this magnitude have never been produced and would be extremely expensive.

The backscatter γ-rays would be detected by a photomultiplier/ scintillator type detector which converts each γ-ray photon to an electrical pulse. The Data Processing Subsystem electronics would determine range by either digitally counting the return rate or integrating the count rate thereby producing an analog

2.0 Low Energy γ-Rays (Continued)

level proportional to the count rate. The γ-ray count rate is a function of the inverse square of the range.

Since range is directly related to count rate, any component drift causing a change in count rate creates a false range indication. Therefore, automatic-gain-control must be employed in the detector together with temperature compensation (or an environmental oven) for the electronics. By using a relatively long half-life radio-isotope source, the source emission can be considered to be constant. Also, no source power is required.

Extreme safety and handling problems would exist for a source of this strength. Special encapsulation and precautions are required to reduce the hazard in case of an accident.

No practical means for rejecting background noise exists. Also, if in the actual flight, lunar dust or rocket exhaust attenuation was significant, erroneous range indications would result.

2.2 Pulsed Isotope Approach

The approach is analogous to the pulsed x-ray approach (pulsed time-of-flight approach) discussed in next section, except that the x-ray tube is replaced with a beta emitting radioisotope, an electron target and a control for modulating the beta flux travel from source to target.

2.2 Pulsed Isotope Approach (Continued)

Hundreds of thousands of curies of beta emitting radioisotopes would be required to obtain the equivalent output of the x-ray tube. Without further discussion, the high source strength makes this approach impractical.

2.3 Pulsed X-Ray Tube

The advantages of radioisotope approach is combined with advantages of radar approach in the pulsed x-ray tube technique. These advantages are as follows:

1) Radiation source strength variation does not affect the time-of-flight measurement technique.

2) Detector sensitivity variations do not affect the system function.

3) Pulse approach allows high peak radiation level required to obtain altitude information, while maintaining low average radiation level.

4) Since the altitude measurement is made during a relatively small portion of time, the system has an inherent noise rejection built into it.

5) Since the x-ray tube is a fail safe device, emitting radiation only when power is applied, the safety and handling problem is minimized.

6) The low energy radiation output of x-ray tube, combined with low average flux level, requires minimum amount of shielding to protect the operating personnel from direct radiation.

3.0 SYSTEM DESIGN SUMMARY

The pulsed time-of-flight measurement concept was selected for use in the NLRTS system. This technique involves emission of short bursts of x-ray at a desired rate. The x-rays travel to the lunar surface and are reflected back to the detector subsystem. The data processing electronics determine the altitude by converting the elapsed time to a representative analog signal and displaying the result on an indicator or meter. The system block diagram is shown in Figure 3.0-1.

The NLRTS performance (accuracy) goals are summarized below:

a) Altitude Range: 0 - 500 feet

b) Altitude Range Accuracy:

   1) 0   - 10 feet: $\pm$ 2% of indicated reading

   2) 10 - 500 feet: $\pm$ 3% of indicated reading

c) Vertical Velocity Range: 1 - 500 ft/sec.

d) Vertical Velocity Accuracy:

   1) 1   -   5 ft/sec.: $\pm$ 1% of indicated value

   2) 5   - 10 ft/sec.: $\pm$ 2% of indicated value

   3) 10 - 100 ft/sec.: $\pm$ 3% of indicated value

   4) 100 - 500 ft/sec.: $\pm$ 5% of indicated value

One obvious problem exists - the altitude error for zero range must not exceed 0 times $\pm$ 2% = 0 error. Therefore, we have assumed a range accuracy goal for 0 - 10 feet of 1 foot which is the practical limit of altitude resolution. One additional comment is in order: For a range indication of zero feet, the NLRTS will be located several feet (we have assumed ten) above the surface
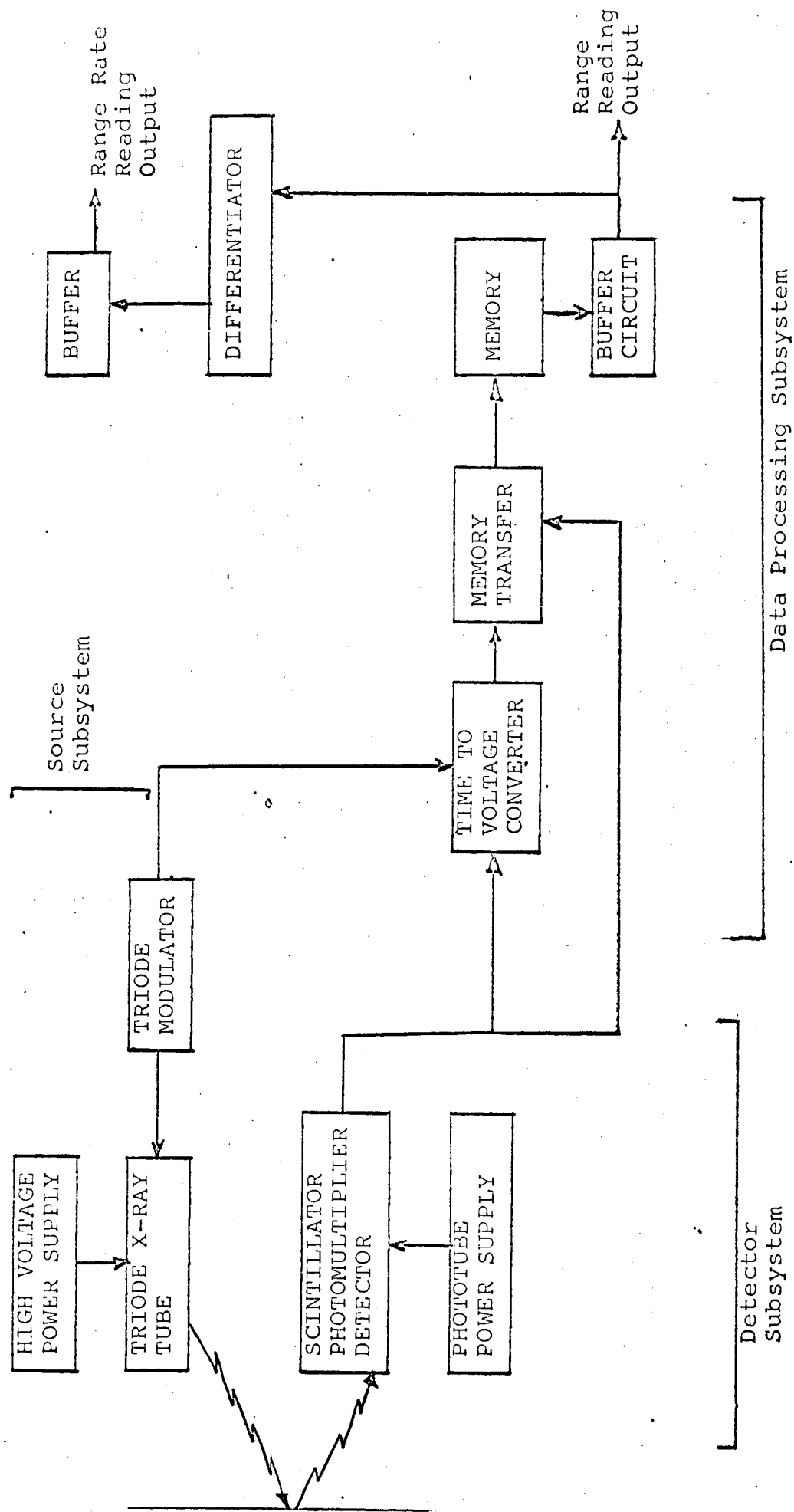
BASIC SYSTEM BLOCK DIAGRAM

FIGURE 3.0-1

3.0 SYSTEM DESIGN SUMMARY (Continued)

since the landing vehicle will probably have legs of one type or another.

The equation governing the x-ray propagation is given below:

$$\frac{I}{I_o} = \underbrace{K_1 \; K_2}_{\substack{\text{Absorp-}\\\text{tion}\\\text{Thru}\\\text{Walls}}} \text{x} \; \underbrace{(1 - \cos \theta)}_{\substack{\text{Loss due}\\\text{to Col-}\\\text{limation}}} \text{x} \; \underbrace{C(\emptyset)}_{\substack{\text{Scatter}\\\text{Factor}\\\text{From}\\\text{Surface}}} \text{x} \; \underbrace{\frac{A_d}{4 \, \pi \, R^2}}_{\substack{\text{Inverse}\\\text{Square}\\\text{Loss}}} \text{x} \; \underbrace{E}_{\substack{\text{Detector}\\\text{Efficiency}}}$$

$\frac{I}{I_o}$ represents the fraction of X-ray flux detected compared to the amount emitted (I_o). K_1 represents the attenuation factor for emitted X-ray caused by the source subsystem housing and the vehicle skin. K_2 represents the attenuation factor for return x-ray caused by the vehicle skin and detector housing. Next, the factor representing the loss due to X-ray beam collimation is given as a function of collimation angle θ. $C(\emptyset)$ represents the scattering factor from the lunar surface which is a function of the scatter angle $\emptyset$. A_d represents the detector area. The flux decreases with the inverse square of altitude. E represents the detector efficiency (effectively unity for the detector used).

The remainder of this section gives an analysis of the x-ray tube emission spectra, the x-ray return versus altitude and a discussion of NLRTS Range and Velocity Errors.

3.1 X-Ray Tube Emission

Electrons from the x-ray tube cathode strike the tungsten target (anode) resulting in a broad Bremsstrahlung emission of x-rays such as that shown in Figure 3.1-1.

The energy conversion efficiency (W) from 100 keV electrons to x-rays is given below:

$$W = \frac{1.98 \ (10^{-4}) \ (1.96E + 2.0) \ Z}{1 + 0.35 \ \log_{10} \ \frac{(82)}{Z}}$$

where

Z = atomic number (tungsten target) = 74

E = electron energy = 0.1 MeV

therefore,

$$W = \frac{\text{X-Ray Energy}}{\text{Electron Energy}} = 0.032$$

The total x-ray energy (E_x) produced is:

$$E_x = 0.032 \ (V) \ (I) \ \frac{1 \ \text{electron}}{1.6 \times 10^{-19} \ \text{coulombs}}$$

For an arbitrary x-ray tube current,

$$E_x = 2.0 \times 10^{16} \ \frac{\text{keV}}{\text{ma} - \text{second}}$$

Distributing this energy over the Bremsstrahlung spectrum of Figure 3.1-1, and calculating the x-ray absorption through the x-ray tube walls, container walls and vehicle skin (assuming a total thickness equivalent to one-half centimeters of aluminum) results in the x-ray spectrum shown in Figure 3.1-2.
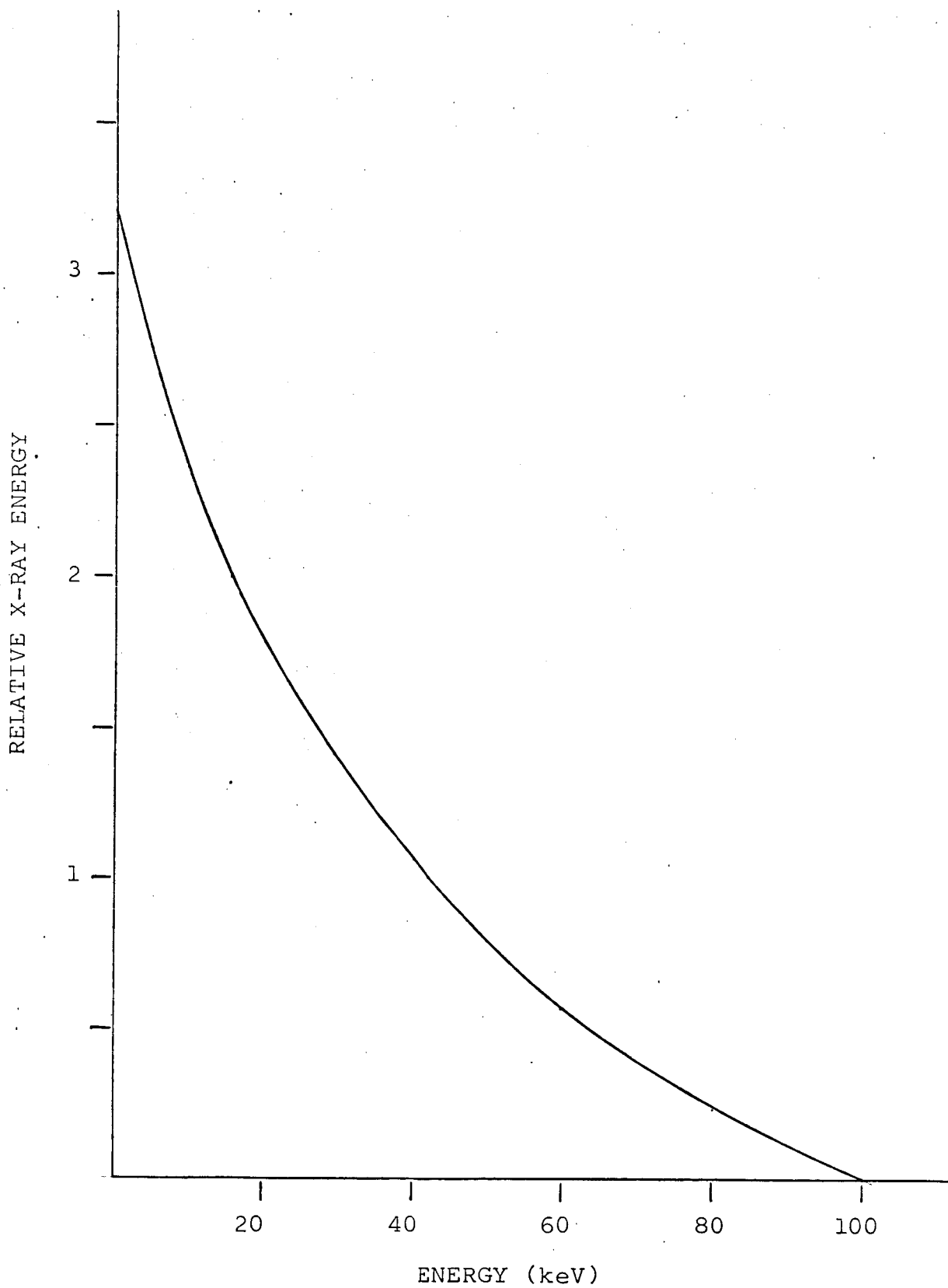
FIGURE 3.1-1

BREMSSTRAHLUNG SPECTRUM FROM
100 keV X-RAY TUBE
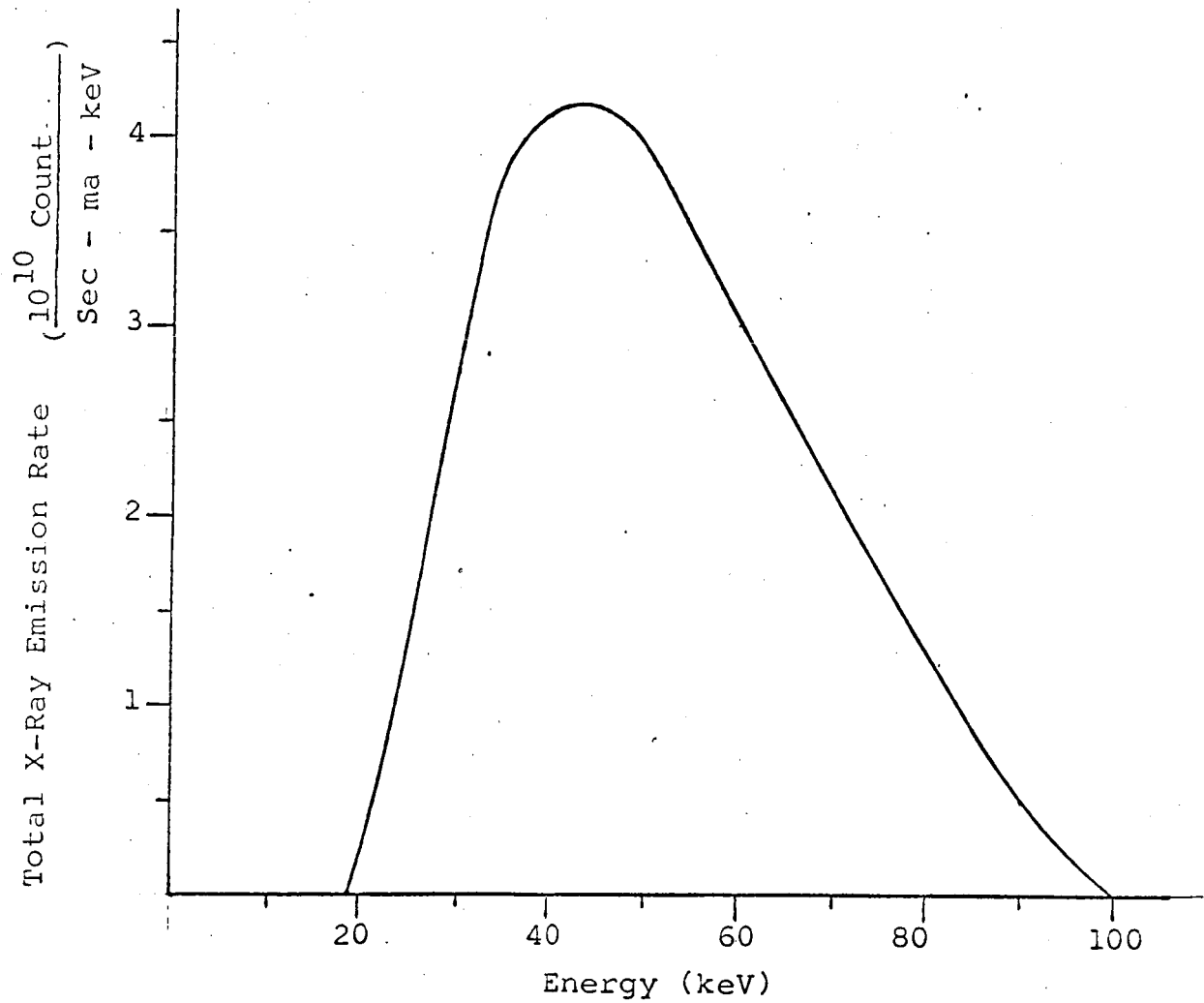
FIGURE 3.1-2

X-RAY EMISSION SPECTRUM

3.2 X-Ray Propagation and Backscatter

The x-ray photons emitted travel along a straight path at the velocity of light as long as no collisions occur. Some scattering will probably occur from lunar dust or the rocket exhaust. However, the resulting attenuation should be negligible as discussed in the proposal. The x-ray tube is essentially a point source of radiation. The percentage x-rays through a collimator angle 2θ (and hitting the lunar surface) is $1/2 (1 - \cos \theta)$ 100%. Of the x-ray photons striking an area $A = \pi R^2 \tan^2 \theta$ of lunar surface, virtually all interact within an inch of the surface if the lunar surface is relatively compact. At the energies involved only two significant types of interactions occur: 1) Photoelectric Absorption and 2) Compton Scatter. Photoelectric absorption involves complete absorption of the photons by ionizing the electrons of the atoms composing the lunar surface. Compton scatter involves a deflection of the incident photon with a corresponding loss of photon energy. Figure 3.2-1 shows the relative intensity and resultant energy of scattered photons. Of those scattering at or near 180 degrees (backscattered) some will hit the detector. The scattering coefficient for average earth has been experimentally determined to be 0.04. Therefore, 4% of the incident x-ray photons lose energy and radiate isotropically (the anisotropy is compensated for in the scattering coefficient). The loss of energy in the Compton scattering process is reflected in the scattered radiation spectrum shown in Figure 3.2-2.

Of the x-ray photons scattered from the lunar surface the number incident upon the detector is proportional to the solid angle

RELATIVE
INTENSITY

ANGLE OF SCATTER (DEGREES)

FRACTION
OF PHOTON
ENERGY
LOST IN
COLLISION

ANGLE OF SCATTER (DEGREES)
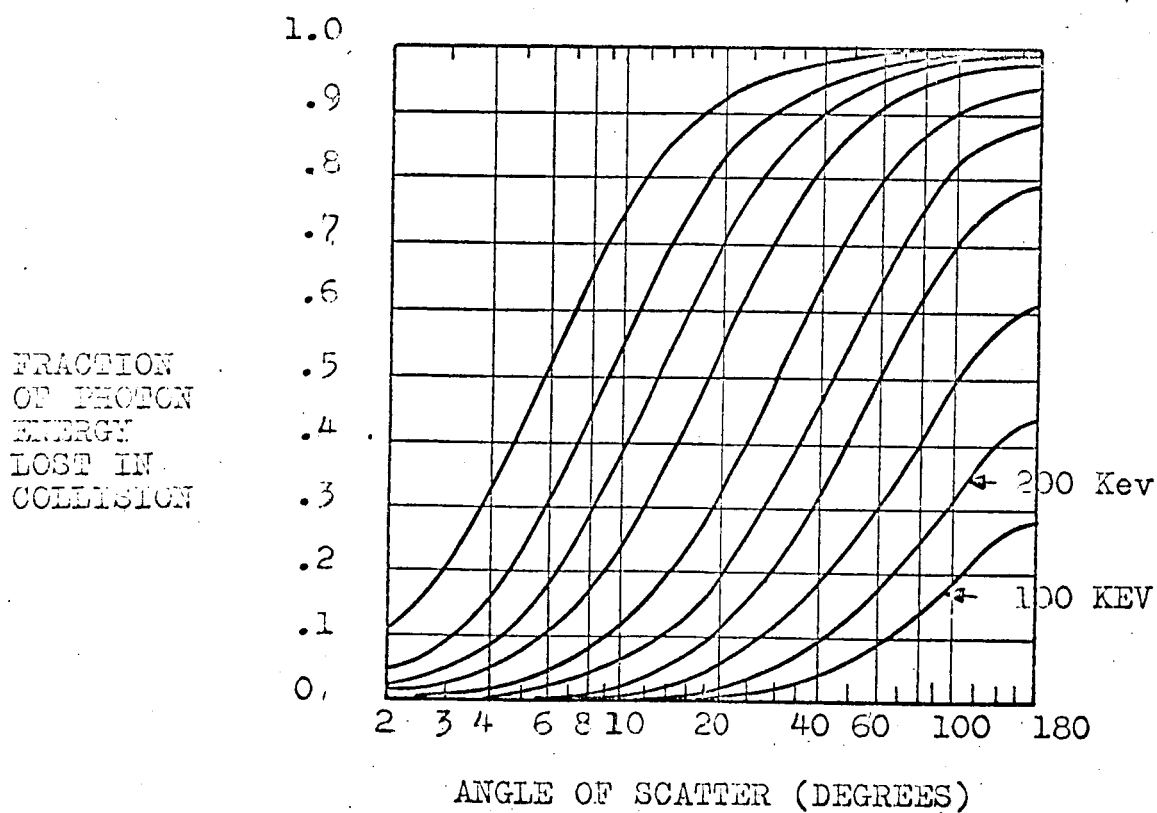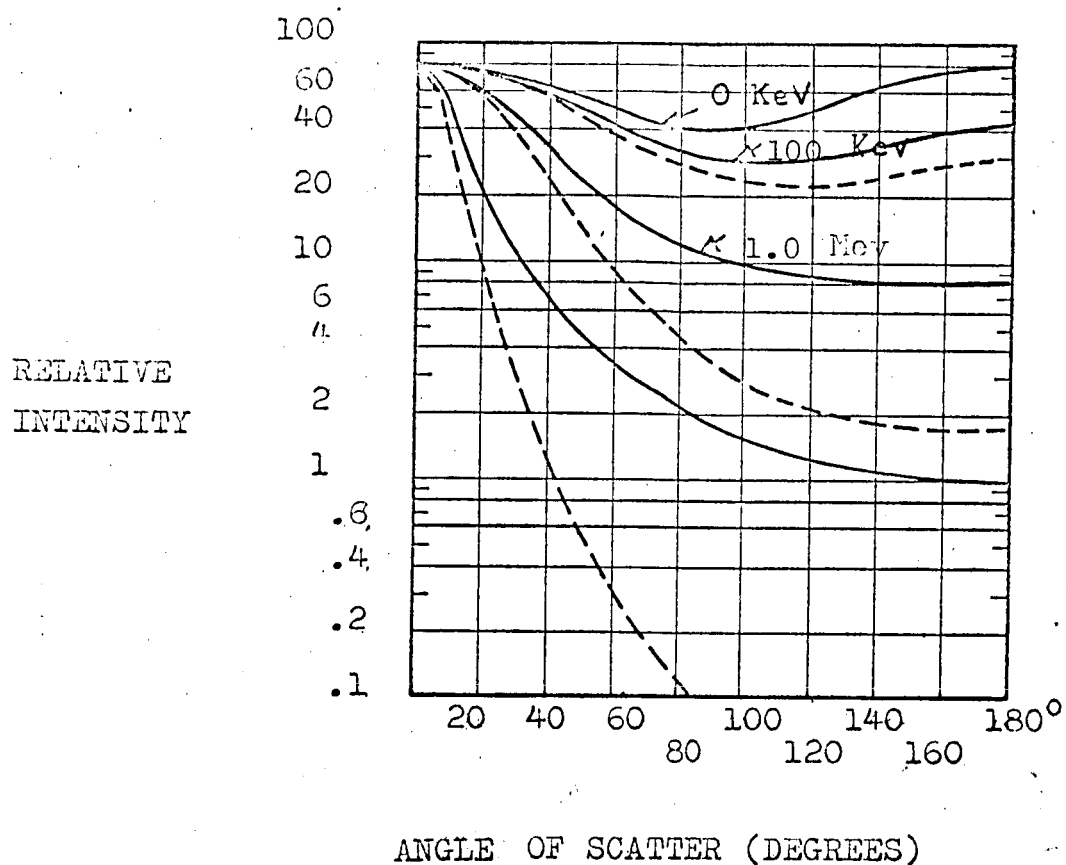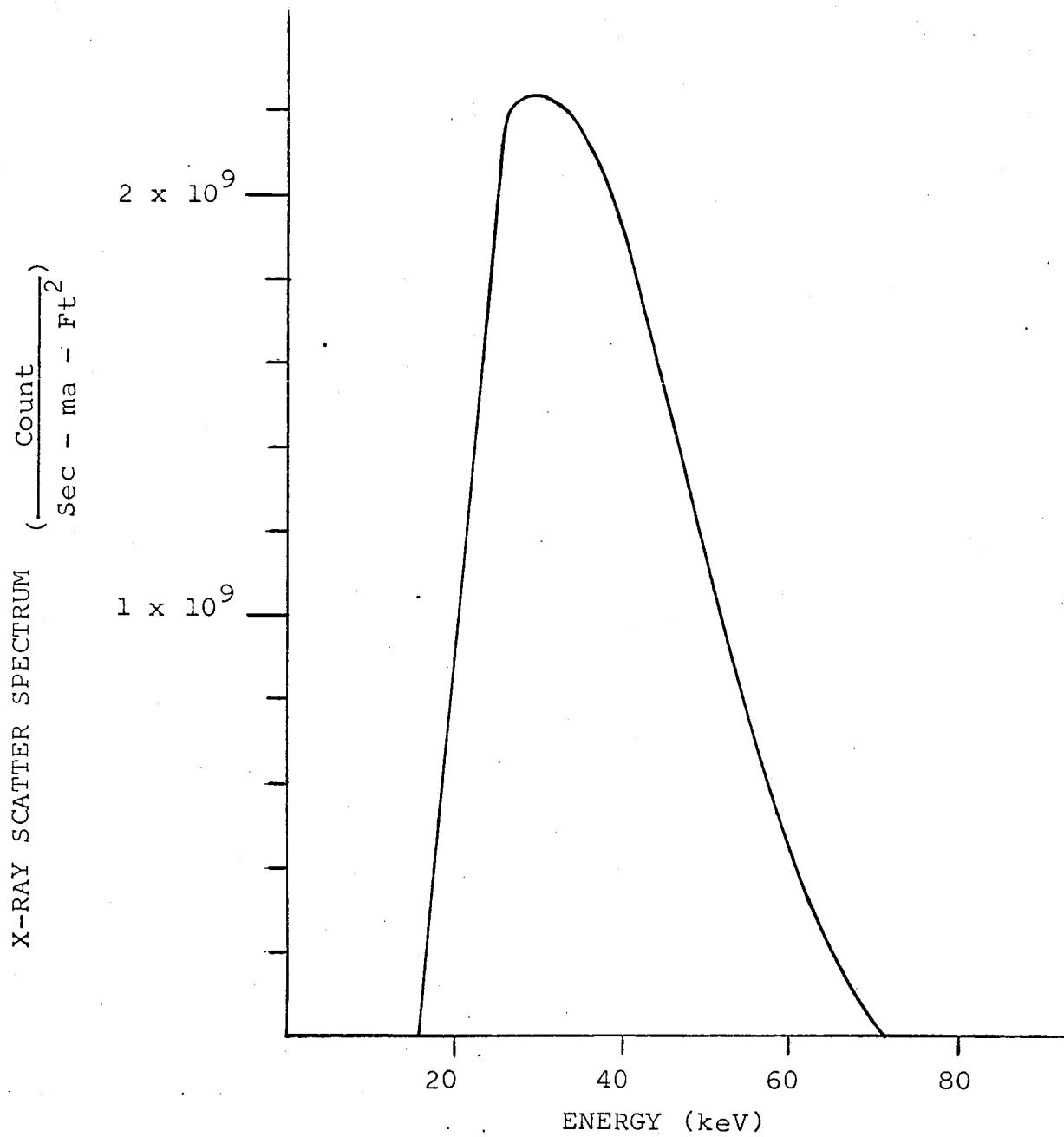
FIGURE 3.2-1

FIGURE 3.2-2

SCATTERED X-RAY SPECTRUM

3.2 X-Ray Propagation and Backscatter (Continued)

subtended by the detector area (A_d). Of those shown in Figure 3.2-2, the number actually detected is reduced by the following factor:

$$\frac{A_d}{2 \pi R^2} \quad E \quad e^{-\mu \rho t}$$

where

$\qquad E \quad = \quad$ detector efficiency

$e^{-\mu \rho t} \quad = \quad$ absorption coefficient of spacecraft skin

$\qquad \mu \quad = \quad$ skin mass absorption coefficient

$\qquad \rho \quad = \quad$ skin density

$\qquad t \quad = \quad$ skin thickness

As in Section 3.1, a skin thickness equivalent to 1/2 centimeters of aluminum will be assumed. The detector efficiency (E) is approximately 99% using a relatively thick Pilot B plastic scintillator. Figure 3.2-3 shows the anticipated detector spectrum. The average rate of x-ray return is given versus range in Figure 3.2-4.

3.3 Pulse Cycle

The simplest pulsed approach is to use a maximum pulse amplitude (peak current) and try to receive a range measurement for every pulse transmitted. However, first the power supply output capacitance cannot store enough energy to supply these giant current pulses. Second, the practical x-ray tubes available (Machlett Labs. ML-645 and Dunlee Corp. Z-170) cannot deliver the required peak currents. Third, in order to maximize tube life and reliability, the x-ray peak current should be minimized. X-ray tube
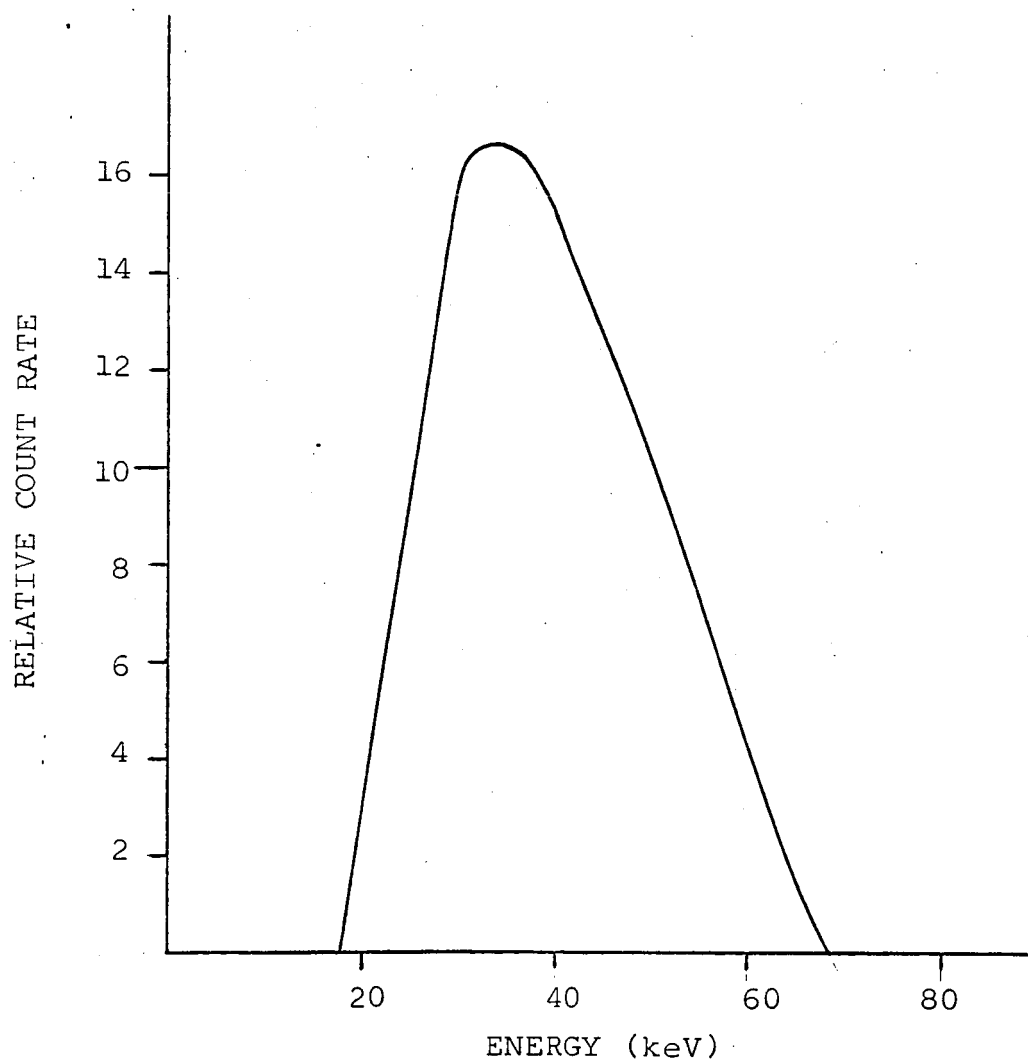
FIGURE 3.2-3

DETECTED X-RAY SPECTRUM
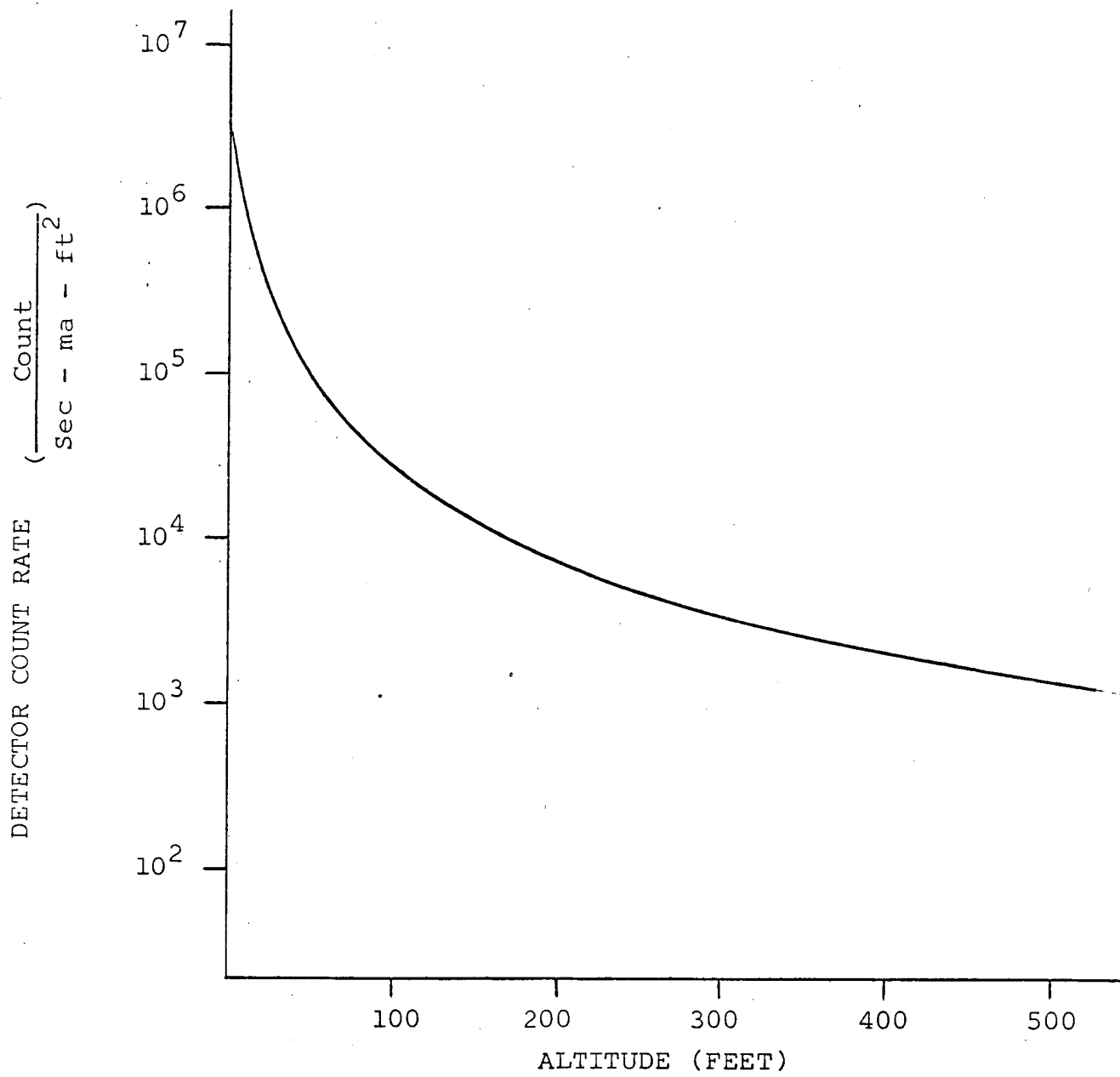
FIGURE 3.2-4

AVERAGE DETECTOR COUNT RATE VS ALTITUDE

3.3 Pulse Cycle (Continued)

life is strongly related to x-ray tube peak current. Lower peak
current does not limit the range capability if multiple pulse and
data storage techniques are employed. Without the use of elabor-
ate cooling of the x-ray tube anode, for the breadboard unit, the
x-ray tube anode dissipation power should not exceed 100 watts.
The pulse cycle relationship is given as follows:

$$100 \text{ watts} = 100 \text{ kv} \times 10 \text{ amp} \times P_{rr} \times t_p$$

where

$$P_{rr} = \text{pulse repetition rate}$$

and

$$t_p = \text{pulse width}$$

The product of P_{rr} and t_p (commonly called the duty cycle) should
not exceed 0.0001. For pulse width of 10 nanoseconds, the maximum
pulse repetition rate is 10 kHz.

A four inch diameter plastic scintillator is used. This provides
a detector area of $A_d = \frac{\pi}{4} (1/3)^2 = 0.090 \text{ ft}^2$. For x-ray tube puls-
es of 10 amp and 10 nanosecond duration, the number of x-ray pho-
tons detected per emitted pulse is given in Figure 3.3-1.

For altitude less than 100 feet, sufficient number of photons are
detected for every pulse emitted. Beyond 300 feet, number of pho-
tons received per pulse becomes quite low, and individual photons
are being detected. Since the data processing electronics can be
triggered by one photon pulse, the range measurement can be made
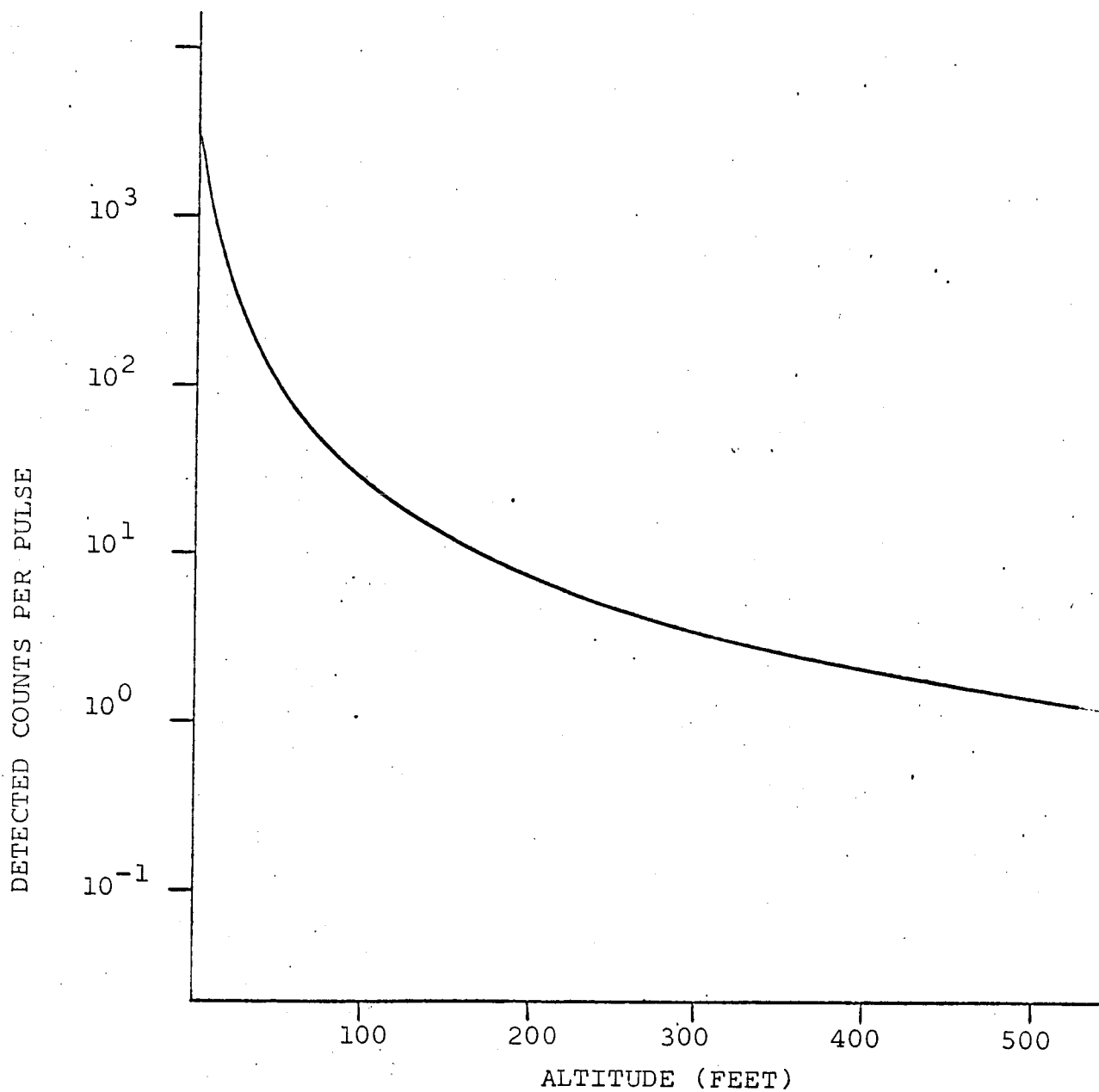
FIGURE 3.3-1

AVERAGE NUMBER OF X-RAY PHOTON
DETECTED PER EMITTED PULSE AS
FUNCTION OF RANGE

3.3 Pulse Cycle (Continued)

up to 500 feet by averaging the measurements over a period of time. The actual time constant used depends upon the anticipated landing profile since the longer the averaging time, the larger the lag error. For low altitude measurement, each pulse emitted results in a range measurement, thus requiring shorter time constant in range measuring circuit. However, for lower velocity, at lower altitude, lag error decreases proportionally. A time constant of 0.5 seconds was selected.

3.4 Ranging Error Analysis

The pulse cycle and expected x-ray return has been discussed. The sources of system errors and their effects will be analyzed. These errors include:

1) Radiation Noise Effects

2) Lag (Velocity) Errors

3) Vehicle Attitude Effects

4) Variable Signal Amplitude

5) Timing and Electronic Errors

6) Photomultiplier Tube Dark Current Noise

.3.4.1 Radiation Noise Effects

Accurate data predicting the radiation background in the lunar
area including particle type and energy is obviously not avail-
able. Radiation noise may cause error if it causes a scintil-
lation in the detector within a period of 10^{-6} seconds after
pulse initiation (represents a range of 500 feet).

For system operating frequency of 10 kHz, the probability of
a given noise pulse causing an erroneous signal during the
time is $10^{-6} \times 10^{4} = .01$.

The effect of noise pulse is to cause an extra triggering of
the range circuit flip-flop. This results in either premature
resetting of range circuit or setting of range circuit flip-
flop after the range information has been received. The first
case occurs only if no range information is received, which can
occur at range greater than 400 feet. This type of error is
averaged with range information in the storage circuit. The
second type of error is rejected in the data processing cir-
cuit, as described in paragraph 6.1. Therefore, only the error
of the first type will be analyzed. The probability of any
noise pulse causing range measurement error is 0.6.

The error caused by the noise has a maximum time of 10^{-6} sec-
onds. For noise count rate of 1000 per second, the probable
number of error pulses is 1000 x .01 x .6 = 6 per second, which
can cause total distance error of 0.15%, when it is averaged
with 4×10^{3} per second signal pulses.

3.4.1 Radiation Noise Effects (Continued)

Data supplied by NASA Goddard to North American Aviation for the Apollo Program is summarized below. Five types of radiation noise may be encountered during a trip to the lunar surface.

a) Residual Radioactivity – The intensity is too low to have an appreciable effect

b) Cosmic Rays – The intensity is too low to have an appreciable effect

c) Van Allen Belt Radiation – No effect at the surface of the moon.

d) Solar Winds – The particle energy, during an active sun, is too low to have an effect. The spacecraft wall will absorb virtually all of them.

e) Solar Flares

1) Solar X-Rays – A class 3 flare which may occur once per week for 15 minutes, may have an intensity of 5×10^5 photons/cm^2 second. The spectral density falls off rapidly below 100 keV and therefore the error source is heavily dependent upon the NLRTS spectrum and the amount of discrimination. The effects of this type of radiation should be updated as more information becomes available.

2) Solar Proton Events – It appears that the high energy protons for a Class I flare may have an appreciable effect for ranges greater than 100 feet. Further study is required regarding the efficiency of the detector to these high energy protons. The use of a window discriminator should cause rejection of the high energy particles.

As more accurate data regarding the intensity and integrated spectra of solar flares becomes available, further analysis should be performed in this area to determine the quantitative effects of solar flare radiation on NLRTS performance at long range.

- 3.4.2 Lag (Velocity) Errors

    A range error results from the delay in measurement and the corresponding change in altitude during that period. At the time of display, the range reading was accumulated over a period (T). The actual range R, and the indicated range R' differ as follows:

    $$R' - R = vT - A\frac{T^2}{2}$$

    where v is the vertical velocity. Using correction techniques, the range indication would be decreased by an amount $\triangle R = \frac{vT}{2}$ making the lag error negligible regardless of the vertical velocity if the knowledge or measurement of velocity is sufficiently accurate.

3.4.3 Variable Signal Amplitude

    The pulses time-of-flight approach is independent of a reasonable change in attenuation and source, detector and electronics variation. These changes include any effects caused by lunar dust and rocket exhaust.

3.4.4 Timing and Electronics Errors

    Variation of the measurement of time is negligible. The only conceivable error would result from charging capacitor and resistor drift with temperature, the ability of the Bilateral Gate and Storage circuits to transfer and storage data, and differential DC amplifier stages to drive the output.

3.4.5   Photomultiplier Tube Dark Current Noise

As with Radiation Noise Effects, the sporatic emissions from the photomultiplier tube photocathode can cause erroneous range indications if they occur during the measurement interval. These noise pulses add with the cosmic noise pulses discussed in Section 3.4.1. For the 56AVP-3 photomultiplier tube, dark current noise plus cosmic noise count rates of 200 counts per second are reasonable.

3.5   Vertical Velocity Error Analysis

The response time for velocity (t_v) should be ten times the measurement interval for Range (5 seconds). Vertical Velocity is measured by differentiating the range measurements. Basically, the slope or the difference in range measurements in a period t_v is a measure of vertical velocity. The landing profile assumed is a constant deceleration profile starting at 500 feet per second at 5000 foot altitude. This represents approximately a 1 g landing profile. The vertical velocity error associated with this technique is illustrated in Figure 3.5-1. The center curve represents the actual range/time landing profile. The upper and lower curves represent the limits of the range measurement error. Plus or minus (R' - R) represents the Range measurement error. $\triangle$ R represents the change in range over a velocity measurement time interval t_v. Illustrated on the left is the minimum and maximum slope realized over a time t_v and a range error R' - R. The slopes $\cup_{max}$
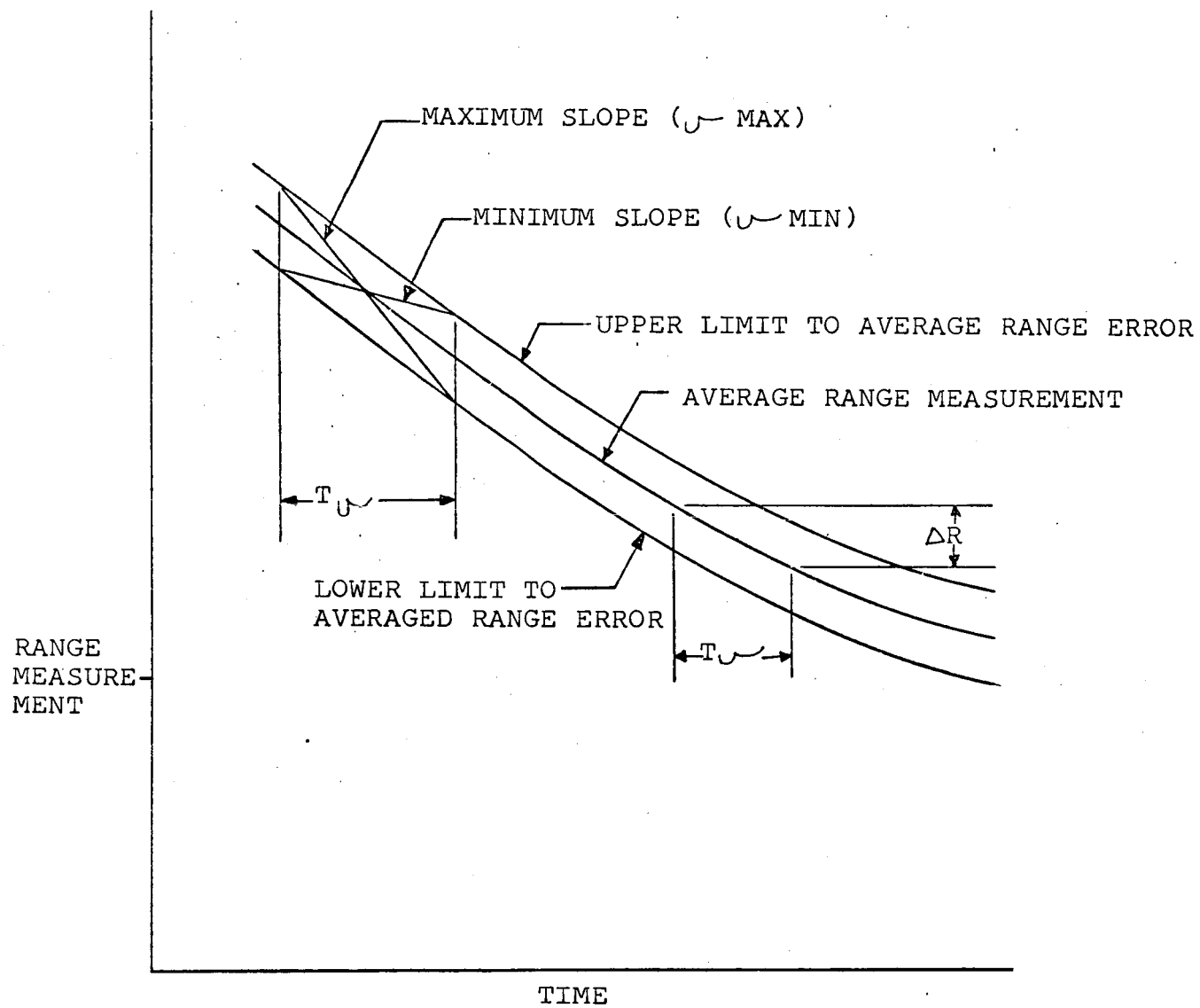
FIGURE 3.5-1

ILLUSTRATION SHOWING LIMITS TO VELOCITY ERROR

3.5   Vertical Velocity Error Analysis (Continued)

and $\widetilde{v}_{min}$ are overemphasized for illustration. The accuracy of vertical velocity measurement can be determined by assuming that the landing craft is motionless. At 500 feet (510 feet from the surface), Vertical Velocity error (V_{max}) could be as large as 5.3 feet per second. Over a measurement time period of 5 seconds this represents a velocity error of approximately 1.06 feet per second. At 300 feet, the Vertical Velocity measurement error could be .64 feet per second. At 100 feet (110 feet above the surface) the root-sum-square error would be 0.26 feet per second. At touchdown (10 feet) the rms error would be 0.12 feet per second.

Vertical velocity calculation (like the range calculation) is based upon an assumed vertical velocity landing profile. The profile assumed is rather steep and the actual would probably be much slower. Therefore, as with the range calculations, the actual error will probably be lower than those shown here. These calculations should be revised upon an anticipated landing profile.

4.0 SOURCE SUBSYSTEM DESIGN

The Source Subsystem provides the x-ray pulses. The x-ray pulses are emitted at a frequency determined by the data processing electronics. The subsystem consists of a triode type x-ray tube, powered by a high voltage power supply and a pulse modulator to drive the x-ray tube. The source schematic is shown in Figure 4.0-1.

4.1 X-Ray Tube

The heart of the Source Subsystem is the x-ray tube which produces the required radiation by a Bremsstrahlung process. This process involves emission of x-rays when electrons are decelerated by collision with a high atomic number material of the anode. In order to obtain the short duration x-ray pulses, a triode x-ray tube is used, allowing high speed control of the electron beam.

The ML-645 tube, manufactured by Machlett Labs., was selected for use in the source because of its high peak x-ray emission. In addition, this tube was specifically developed to meet severe environment conditions encountered by space flight equipment. An outline of the tube is shown in Figure 4.1-1. The grid-cathode structure of the tube is identical to a standard microwave planar triode tube, thus assuring high speed pulse capability. The tube is capable of providing peak plate current up to 20 amperes, at high filament voltage and reduced

C4-C10 .001 µf

R4-R11 2CHT4?

B

A

C1
.1

R1
1K

Q1
2N3446

C3
.01

T1

CR1
1N4001

C2
10µ

R2

R3

Q2
2N3446

R4
771

CR2
1N4001

CR3

Q3
MHT334

Q4
MHT334

T2
7503

CR11

CR?

Lewis Grayson

NLRTS

FOLDOUT FRAME 1   30
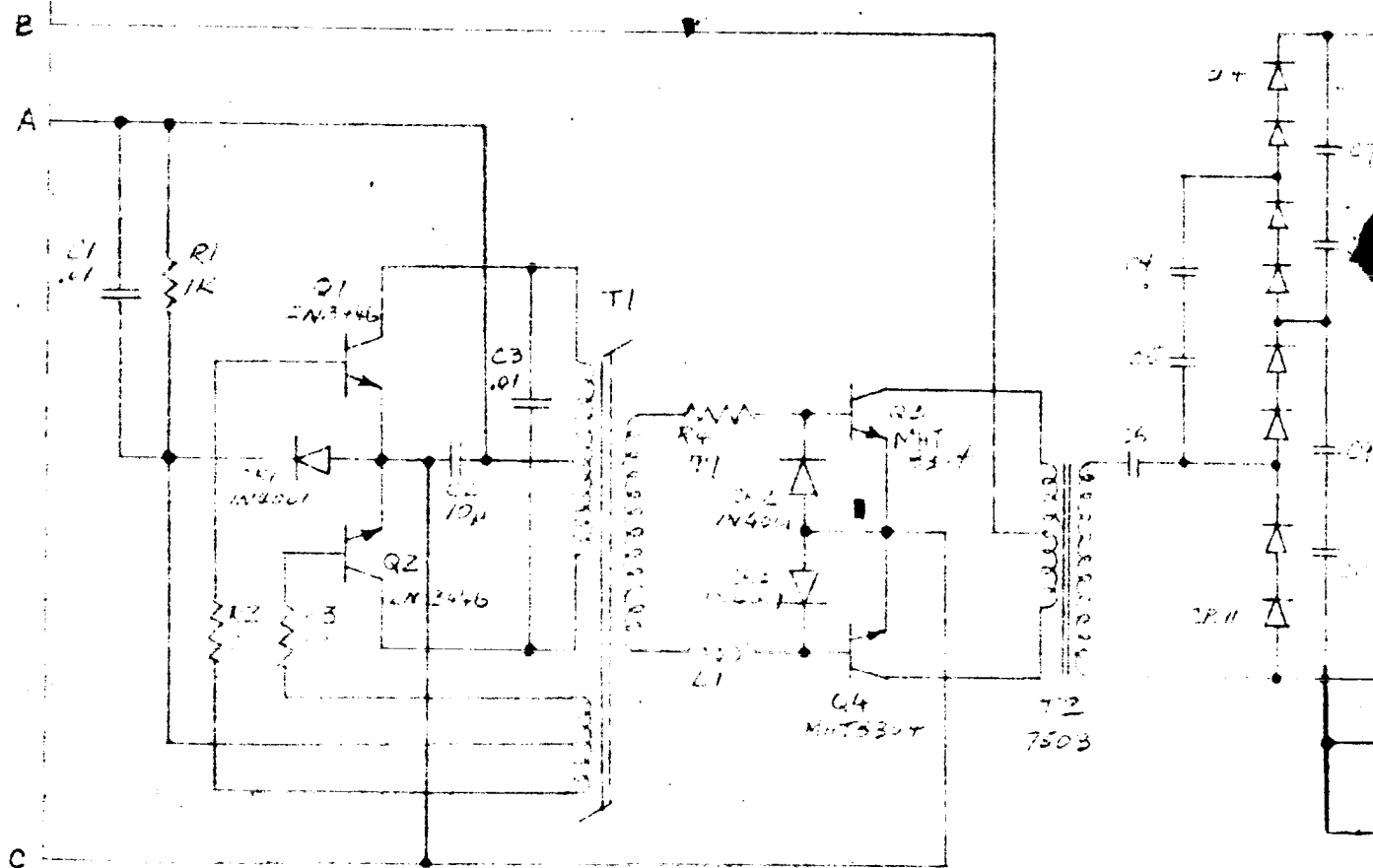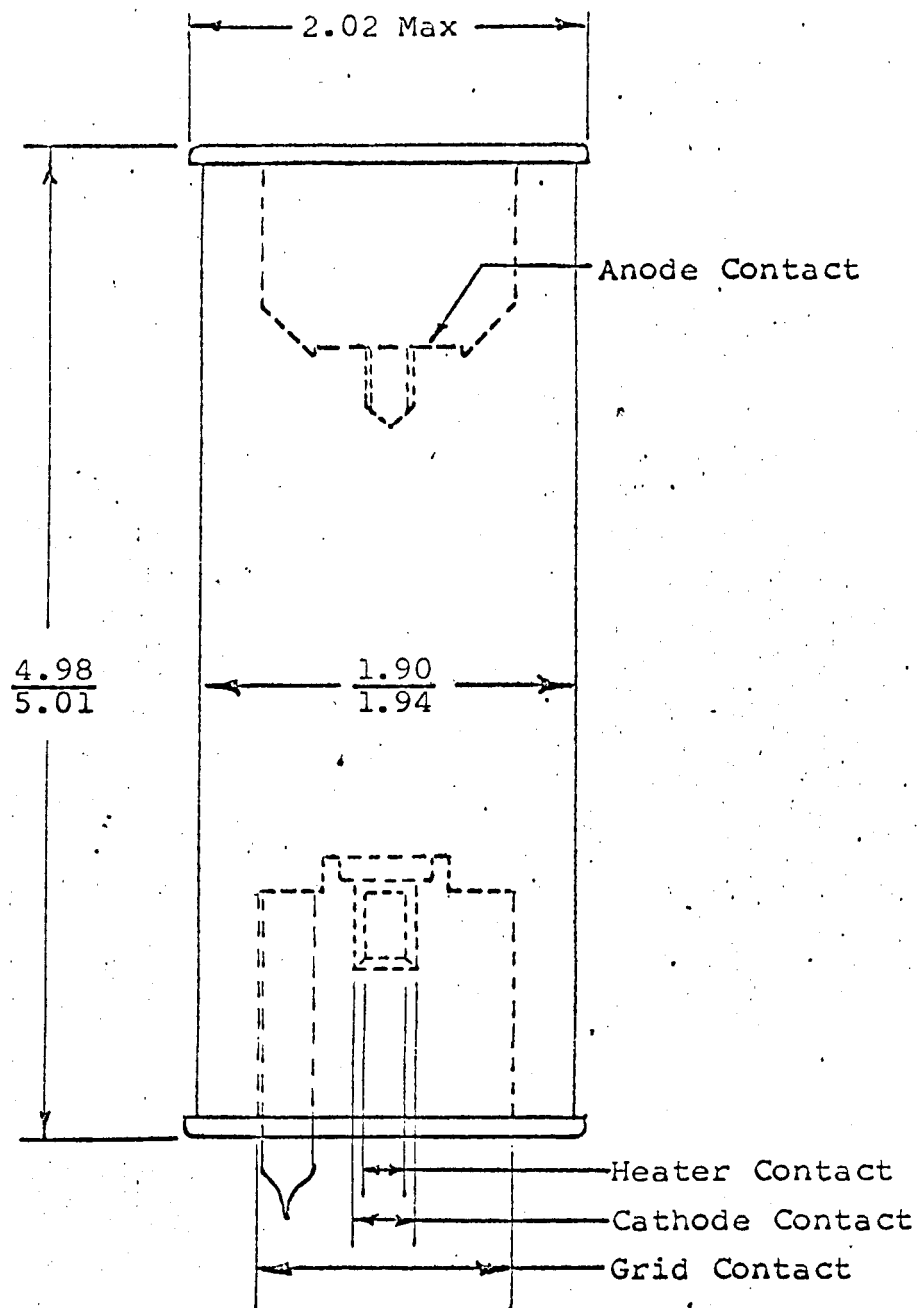
FIGURE 4.0-1

FIGURE 4.1-1

OUTLINE OF X-RAY TUBE

ML-645

4.1 X-Ray Tube (Continued)

tube life. Nominal operation will provide 10 ampere peak current.

The anode on the ML-645 is a flat anode and emits an emission pattern as shown in Figure 4.1-2. In order to provide an emission pattern which is perpendicular to the source housing, the tube is mounted into the source housing at an angle, as shown in Figure 4.1-3.

The operating voltage of the x-ray tube is limited to 100 kilovolt for the present model. The voltage rating of the tube is 100 kV with probable operation at 125 kV. Operating above 125 kV is not considered practical at this stage of tube development.

4.2 Power Supply

Design, packaging and assembly of the high voltage power supply was one of the critical items in the program. A state-of-the-art supply is used to minimize weight and volume. The DC supply is required to produce 100 kilovolt at 1 milliamperes average current, with peak pulse current of 10 amperes. The DC supply was chosen over the AC type because of its capability to provide high pulse current and capability to provide x-ray pulse at high repetition rate.

LINE OF
MAXIMUM ENERGY

BEAM CROSS
SECTION
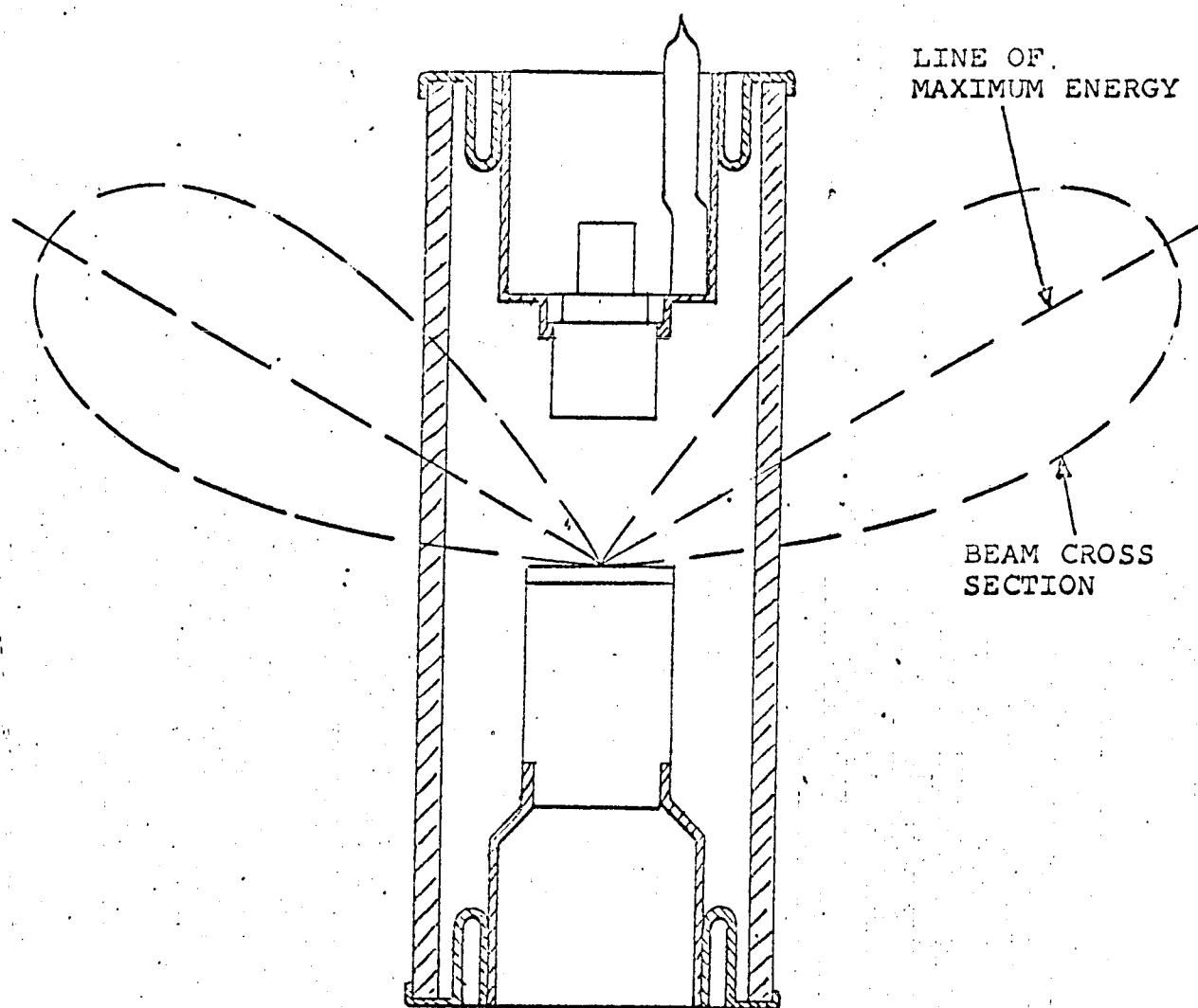
FIGURE 4.1-2

X-RAY BEAM PATTERN
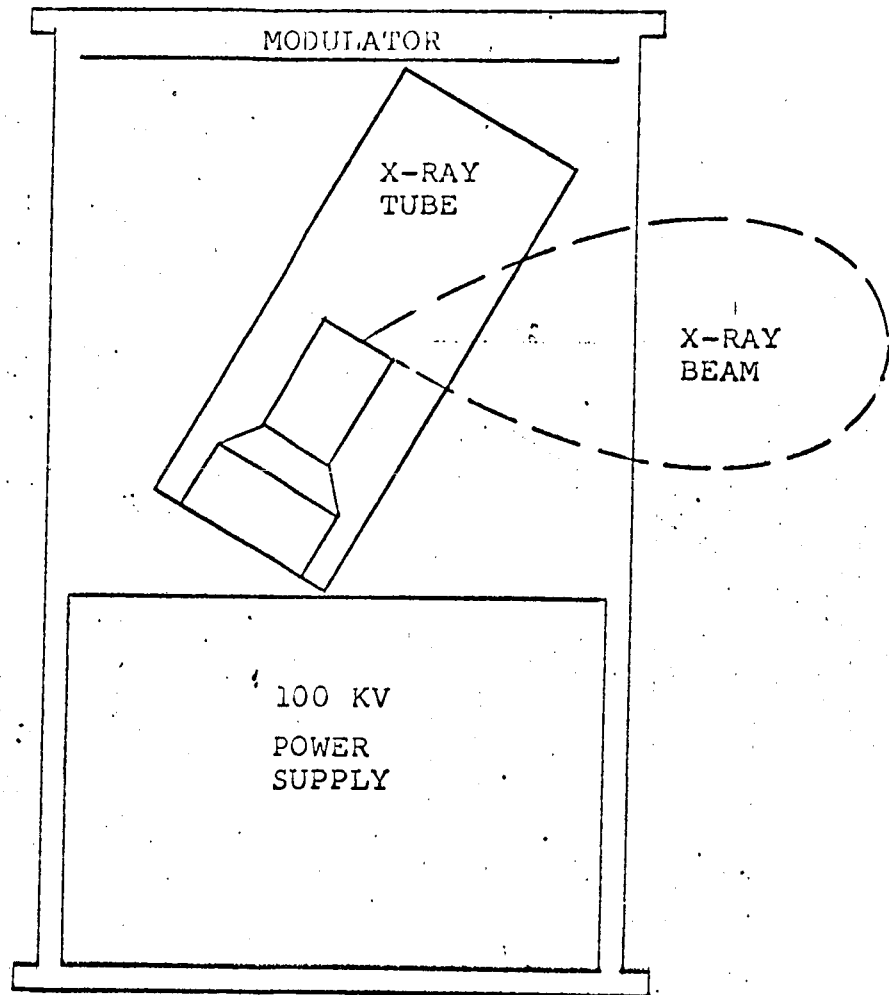
FIGURE 4.1-3

SOURCE ASSEMBLY LAYOUT

4.2 Power Supply (Continued)

The power supply converts the 28V DC ship power to required

high voltage. The block diagram of the supply is shown in

Figure 4.2-1.

4.2.1 Oscillator - Driver

The square wave oscillator converts the DC voltage into AC

voltage at frequency of approximately 4.2 kHz. The oscilla-

tor is an over-driven push-pull transformer coupled transistor

oscillator. The magnetic core transformer is used as timing

element in order to provide a symmetrical square wave under

all load conditions. A resistor - diode starting circuit en-

sures proper circuit operation whenever power is applied. The

oscillator stage is designed separately from the power conver-

ter stage in order to allow frequency selection independent of

high voltage transformer design.

The output of the oscillator transformer drives the power con-

verter stage. The power switching transistors are required to

handle peak current up to 20 amperes.

4.2.2 Transformer

The high voltage step-up transformer was designed and fabricat-

ed by EDCO Systems Inc., Santa Clara, California, in coopera-

tion with General Nucleonics personnel. The problem in designing

a transformer for this power supply is to provide a high turn

28 V DC
Power

```
           ┌──────────────────────┐
           │      REGULATOR       │
           └──────────────────────┘

  ┌──────────────────┐      ┌──────────────────┐
  │                  │      │   HIGH           │
  │   OSCILLATOR     │─────▶│   POWER          │
  │                  │      │   DRIVER         │
  └──────────────────┘      └──────────────────┘

                      ┌──────────────────────┐
                      │      STEP-UP          │
                      │    TRANSFORMER        │
                      └──────────────────────┘

                      ┌──────────────────────┐
                      │     RECTIFIER         │
                      │     MULTIPLIER        │
                      └──────────────────────┘
```

100 KiloVolt
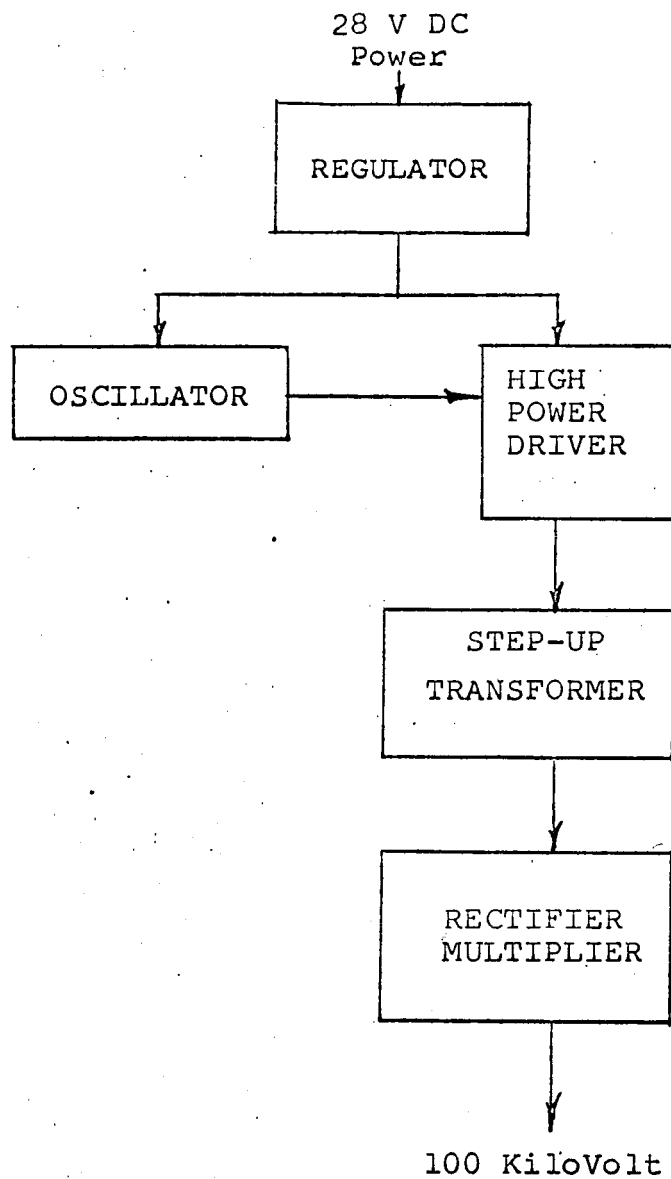
FIGURE 4.2-1

BLOCK DIAGRAM — HIGH VOLTAGE SUPPLY

4.2.2   Transformer (Continued)

ratio with minimum interwinding capacitance and high voltage
insulation, while maintaining minimum size and weight.

The output - input ratio requirement of 27500 volt : 24 volt
constitutes a 1150:1 turns ratio. Thus, the distributed in-
terwinding capacitance is reflected to the primary by a factor
of 1,300,000 and the interwinding capacitance becomes a very
critical problem. The capacitance is minimized by dividing
the secondary into six sections of narrow width layers. This
method of winding also decreases interlayer insulation require-
ments.

The transformer winding is impregnated with an epoxy compound
for rigidity and additional insulation. The prototype trans-
former weighs 592 grams (1 lb. 5 oz) and occupies a space of
3 inches x 3 inches x 3.5 inches.

4.2.3   Multiplier

The AC output of the high voltage transformer is multiplied,
rectified and filtered into a DC voltage by the Cockcroft-
Walton multiplier circuit. A tradeoff study was performed for
transformer output requirement versus multiplier component
number and rating requirement. The present state-of-the-art
dictated the optimum configuration as a transformer with 50
kV peak to peak output with a quadrupler.

4.2.3   Multiplier (Continued)

The assembly of the multiplier must consider high voltage in-
sulation and corona problems. The insulation media for the
prototype unit is sulfur-hexafluoride gas, with dielectric
strength of approximately 200 volts per mil. The multiplier
assembly includes the high voltage transformer and makes maxi-
mum usage of the 8 inch diameter cylinder housing, allowing
large safety margin on critical voltage stress points.

4.3   Modulator

The x-ray tube grid must be pulsed into positive region in or-
der to obtain the peak anode current of 5 to 10 amperes. The
ML-645 tube requires a bias of -100 volt for cutoff and +300
volt bias during pulse. The grid input presents a nonlinear
load to the modulator, drawing a peak current of approximately
1 ampere at +300 volt drive.

The pulse modulator circuit must have a low output impedance.
An avalanche transistor circuit was chosen for its high cur-
rent capability, fast clean pulse output and relative high
efficiency. The high output is derived by stacking four trans-
istors in series, to obtain a 120 volt pulse, then multiplying
the pulse in a 4 to 1 step-up transformer. The pulse shape and
width is determined by the time constant of the delay line in
the avalanche circuit.

The delay line is charged to a voltage which is the sum of the
breakdown voltages of each avalanche transistor. When the

4.3 Modulator (Continued)

first transistor is triggered by a pulse from the data process-
ing electronics, the avalanche action of the first transistor
triggers avalanche breakdown in the other transistors. When
the transistors avalanche, the energy stored in the lumped con-
stant delay line is dumped into the load. This transfer of
energy is accomplished in twice the delay time of the line.
After the energy has been transferred, the transistors are
turned off due to lack of sustaining current. The circuit is
then disabled, i.e., unable to produce a pulse, until the de-
lay line has been charged up again. This dead time is approx-
imately 50 μ sec.

5.0 DETECTOR DESIGN

The x-ray signal must be detected and converted into an analogous electrical signal before the data processing electronics circuits can properly analyze the signals.

The x-ray energy is first converted to a light energy in the scintillator. The light energy is then converted into electrical pulses by the photomultiplier tube photocathode and amplified in the photomultiplier tube. The output of the detector is transmitted to the data processing electronics by coaxial cable. The schematic is shown in Figure 5.0-1.

5.1 Scintillator

The x-ray energy must be detected with a very short response time to be able to measure time differences in order of few nanoseconds. A plastic scintillator was selected to meet this requirement.

The scintillator, 4 inches in diameter x 4 inches in length, was selected to provide optimum collection efficiency at the energies involved.

5.2 Photomultiplier Tube

The light output of the scintillator must be detected and amplified without introduction of excessive noise pulses.

-2300 Volt   1 Meg

18K

470K
1W

240K
½W

150K

160K

120K

120K   56 AVP/03

120K   Amperex

120K

120K

120K

120K   .001

120K   .001

120K   .001

120K   .01

120K   .01

Signal
Output

FIGURE 5.0-1

DETECTOR SCHEMATIC

5.2 Photomultiplier Tube (Continued)

Type 56AVP-3 photomultiplier tube, manufactured by Amperex, was selected for its high gain and low noise characteristic. This tube also has a fast response time required for nanosecond time resolution.

The two inch diameter tube is placed in a magnetic shield tubing to prevent magnetic field effect on operation of the tube. The face of the tube is coupled to the scintillator with a light coupling compound, Dow Corning 20-057, to obtain optimum coupling of light. The photomultiplier tube is mounted in light tight housing. The tube surface to scintillator contact is maintained by spring pressure at base of the tube. The dynode voltages are supplied by the resistor divider string, mounted in the tube socket.
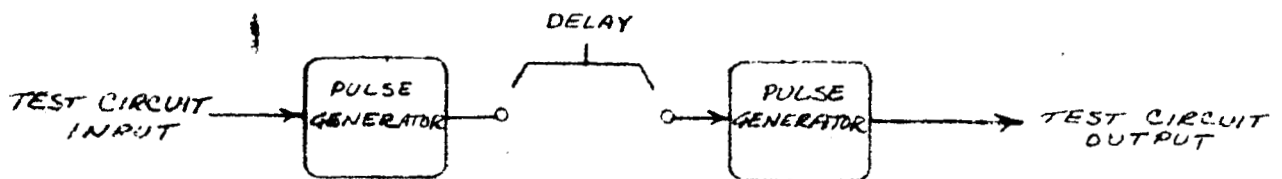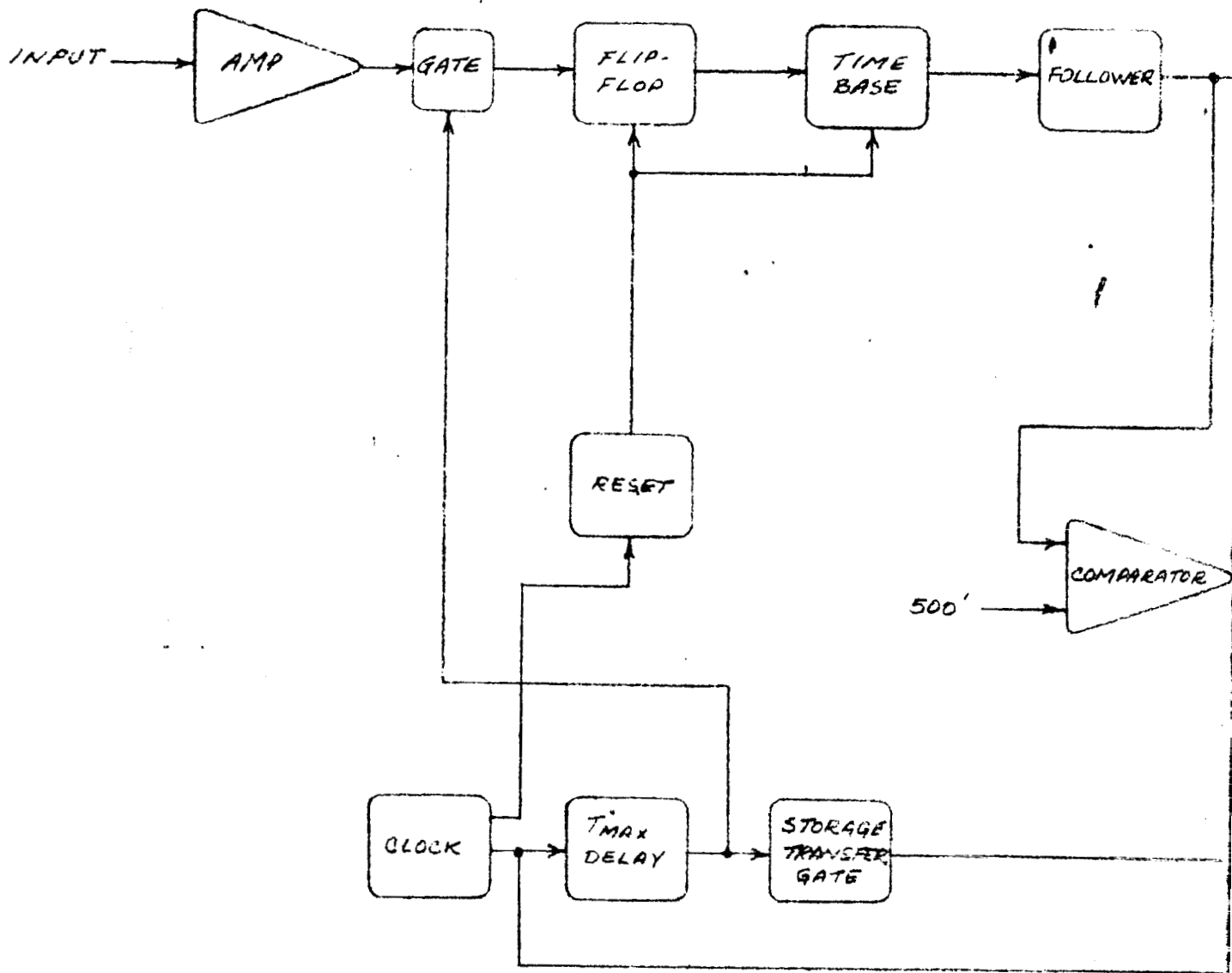
6.0 DATA PROCESSING ELECTRONICS

The information derived from the x-ray transmission must be analyzed and processed to obtain altitude and velocity data. This is the main function of the data processing subsystem. In addition, the subsystem includes power supply required for various circuits, switches for on-off control of system, and display meter for range and velocity information.

6.1 Range Circuit

The block diagram of the range and velocity circuit is shown in Figure 6.1-1. A detail schematic is given in Appendix A.

The range circuit performs the function of measuring the time between a "zero range return" from the skin of the vehicle and x-ray photon return from the lunar surface. This time interval, which is a direct measure of altitude, is converted into a DC voltage and displayed on a meter.

The system pulse repetition rate is controlled to 10,000 pulses per second by a free-running multivibrator clock. Each clock pulse initiates two functions: 1) trigger the x-ray tube modulator circuit, and 2) triggers a maximum range time delay (T_{max}) gate circuit. This gate is 1.3 μ sec long and allows detector signal to be analyzed only during this period. Any signal occurring outside of this period is considered to be noise pulse, and is prevented from affecting the range measuring circuit.

INPUT → AMP → GATE → FLIP-FLOP → TIME BASE → FOLLOWER

RESET

COMPARATOR

500'

CLOCK → T_MAX DELAY → STORAGE TRANSFER GATE

DELAY

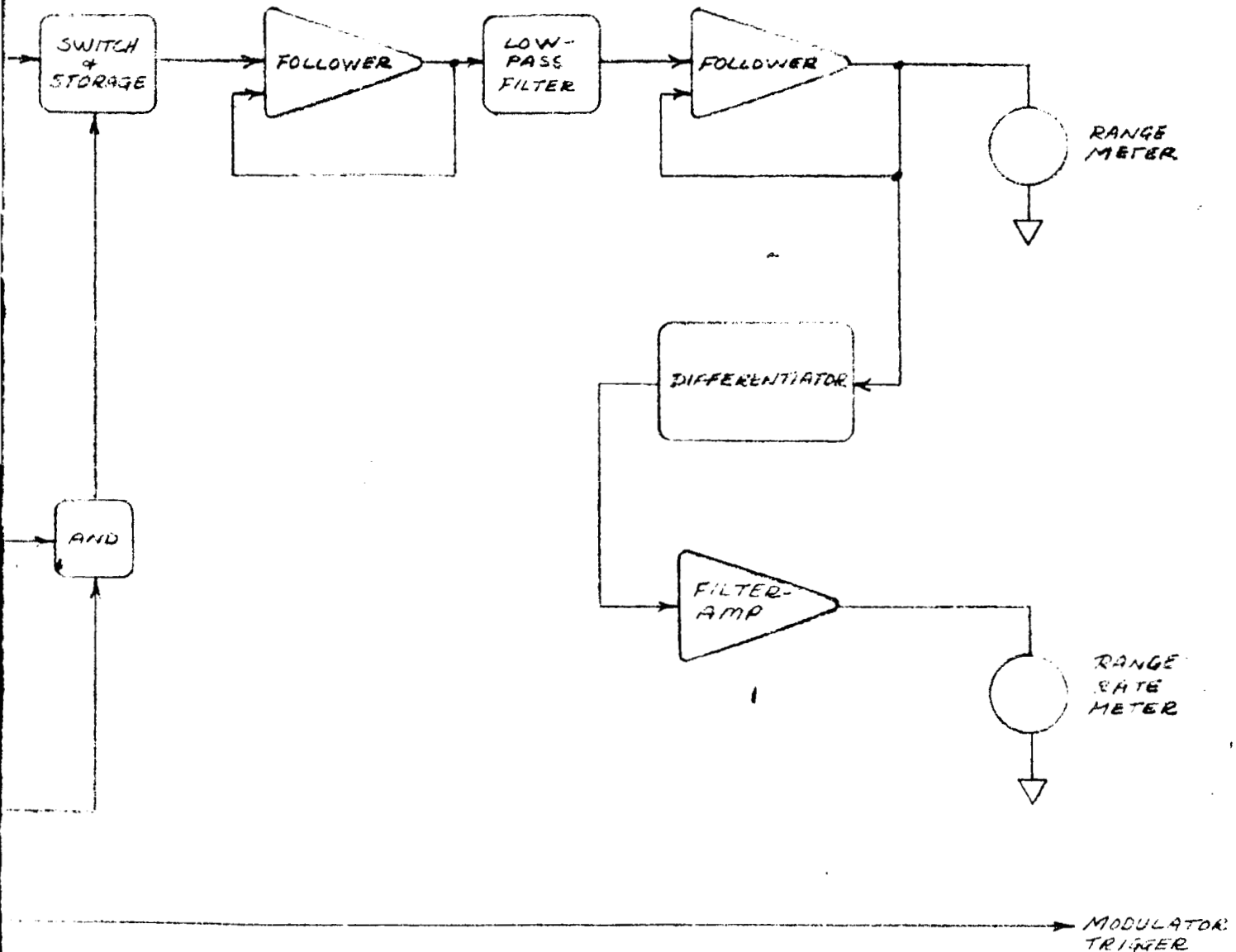TEST CIRCUIT INPUT → PULSE GENERATOR →○   ○→ PULSE GENERATOR → TEST CIRCUIT OUTPUT

FIGURE 6.1-1

NLRTS
RANGE & RANGE RATE
CIRCUIT
BLOCK DIAGRAM

6.1 Range Circuit (Continued)

Upon emission of x-ray pulse, a scattered pulse from vehicle skin is immediately detected. This pulse is amplified and sets the flip-flop which in turn starts the time base circuit. The second pulse will be the return from the lunar surface. This pulse resets the flip-flop and stops the time base circuit. A voltage proportional to range now exists in the time base circuit. At the end of maximum time delay gate, the range information is transferred to the storage circuit through the transfer switch, provided the time base circuit has not exceeded the maximum range voltage. If the maximum range voltage has been exceeded, it is assumed that return pulse from lunar surface was not detected, and therefore information in time base circuit is not valid. The comparator circuit detects any invalid signal and inhibits the transfer pulse through the AND gate. A reset pulse is used to return the flip-flop and time base circuit to proper initial condition prior to start of next clock pulse. The information in the storage circuit is displayed on a meter. The range output is scaled to 1 volt per 100 feet.

The pulse amplifier, Q1 - Q2, circuit provides gain of 10 for the input signal. The gate, Q3, shunts the signal to ground except during the time interval controlled by time delay circuit Z2. The tunnel diodes, CR1 and CR2, and associated circuitry form a high speed flip-flop to convert the time interval to a pulse width, with minimum time of 10 nanoseconds. The time base circuit consists of constant current generator, Q9, and charge

6.1 Range Circuit (Continued)

capacitor, C17. The constant current is adjusted to give 5 volt

per microsecond charge rate on capacitor. The output of charge

capacitor is buffered by high impedance FET circuit, Q13, in or-

der to minimize error due to external discharge. The data trans-

fer switch uses a MOS-FET, Q15, for high impedance isolation of

storage capacitor, C24. The dual MOS-FET, Q16, is used after

storage capacitor for high impedance load of capacitor and low

drift differential amplifier. The low pass network, R83 - C29,

filters any rapid change or ripple on the range information.

The timing of all system signals are initiated by the multivi-

brator, Q4 - Q8. The clock pulse initiates a gate circuit, Z2,

which allows signal processing for 1.3 microseconds. This in

turn initiates a 15 microsecond gate which controls the data

transfer switch, through AND gate, Q20 - Q18, in conjunction with

comparator, Z1. The comparator analyzes the time base circuit

output and if it exceeds 5 volts, inhibits the AND gate. Be-

tween clock pulses, the reset circuit, Q7 - Q10, resets the

flip-flop and charge capacitor, to their respective initial

starting conditions.

6.2 Range Rate Circuit

The velocity information is obtained by differentiating the

range information. The amplifier, Z5, differentiates the range

information, at time constant of 0.1 seconds. The amplifier, Z4,

provides the proper scale factor, 1 volt per 100 feet per second,

and also filters the output of differentiator, at 1.6 second

time constant.

6.3 Test Circuit

A test circuit, useful for calibration of the data processing electronics, is included in the subsystem. Using the modulator trigger signal, the test circuit provides a double pulse signal to simulate the expected detector output.

The modulator trigger pulse is fed into amplifier, Q5, which provides an inverted and non-inverted signal. The inverted signal is routed to the test signal output mixer circuit. This pulse simulates the zero range pulse from the detector. The non-inverted signal is delayed by any desired time and then inverted by output amplifier, Q11. This second pulse is mixed in the output circuit and simulates the lunar surface return signal.

6.4 Power Supply

The system primary power, 28 volt dc, is converted to various voltages for operation of electronic circuits by the solid state DC-DC converters. Commercially available, off-the-shelf items were used to expedite design of the system. The voltage level required, power consumed and power supply part numbers are listed in Table 6.4-I.

6.5 Calibration

The data processing electronics require calibration as outlined in Appendix B. The detector and source subsystems do not require calibration.

TABLE 6.4-I

DC-DC CONVERTER DATA

FUNCTION	VOLTAGE	POWER	POWER SUPPLY	
Electronic Circuit	± 15 Volt	5 watts	9584121	(1)
X-Ray Tube Filament	8 Volt	12 watts	AL6D-7.9A	(2)
X-Ray Tube Bias	300 Volt	0.2 watts	9584112	(1)
Modulator Supply	1000 Volt	1 watt	9583114	(1)
Detector Supply	2000 Volt	1.75 watts	9567116	(1)

(1) Manufactured by Transformer Electronics Company

(2) Manufactured by Abbott Transistor Labs. Inc.
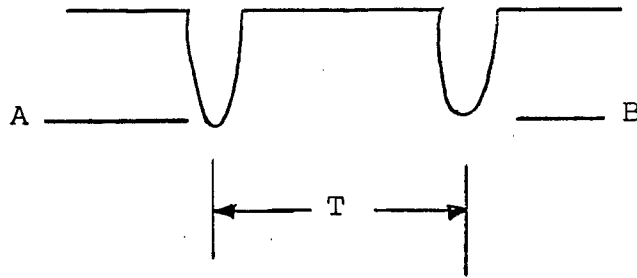
7.0 TEST RESULTS

The NLRTS system design is based on low atmospheric attenuation of the radiation. In order to provide the proper test condition for a functional test, the 60 foot sphere altitude chamber facility of NASA, at Langley Research Center, Hampton, Virginia, was utilized. Due to the size of the chamber, maximum altitude simulated was 50 feet. Preliminary test indicated that one-tenth atmospheric pressure (80 mm mercury) was sufficiently low to have negligible attenuation effect on radiation.

The illustration of Figure 7.0-1 shows the test setup. The floor of the chamber was lined with plywood to obtain reflection coefficient similar to ground. The normal steel floor would have much smaller reflection coefficient. The cable suspending the system was marked at 10 foot intervals, for visual altitude reference.

The first test, performed on 6 November through 9 November 1967, resulted in   malfunction of data processing electronics. The cause was later determined to be extraneous pulse resulting in undesired triggering of the range circuit. The detector output signal was observed on a scope to verify the existence of proper signals. The result is given in Table 7.0-I. The result shows the expected time relation (2 nanosecond per foot) and that the signal amplitude is inversely proportional to the distance.

```
┌─────────────────────────────────────────────────────────────────────┐
│                        TABLE 7.0-1                                    │
│                                                                       │
│                    DETECTED SIGNAL WAVEFORM                           │
└─────────────────────────────────────────────────────────────────────┘
```

Height (Feet)	Amplitude A (Volt)	Amplitude B (Volt)	Time T (Nanosecond)
50	2	1.0	100
40	2	1.0	80
30	2	1.3	60
20	2	2	40
10	2	3	20

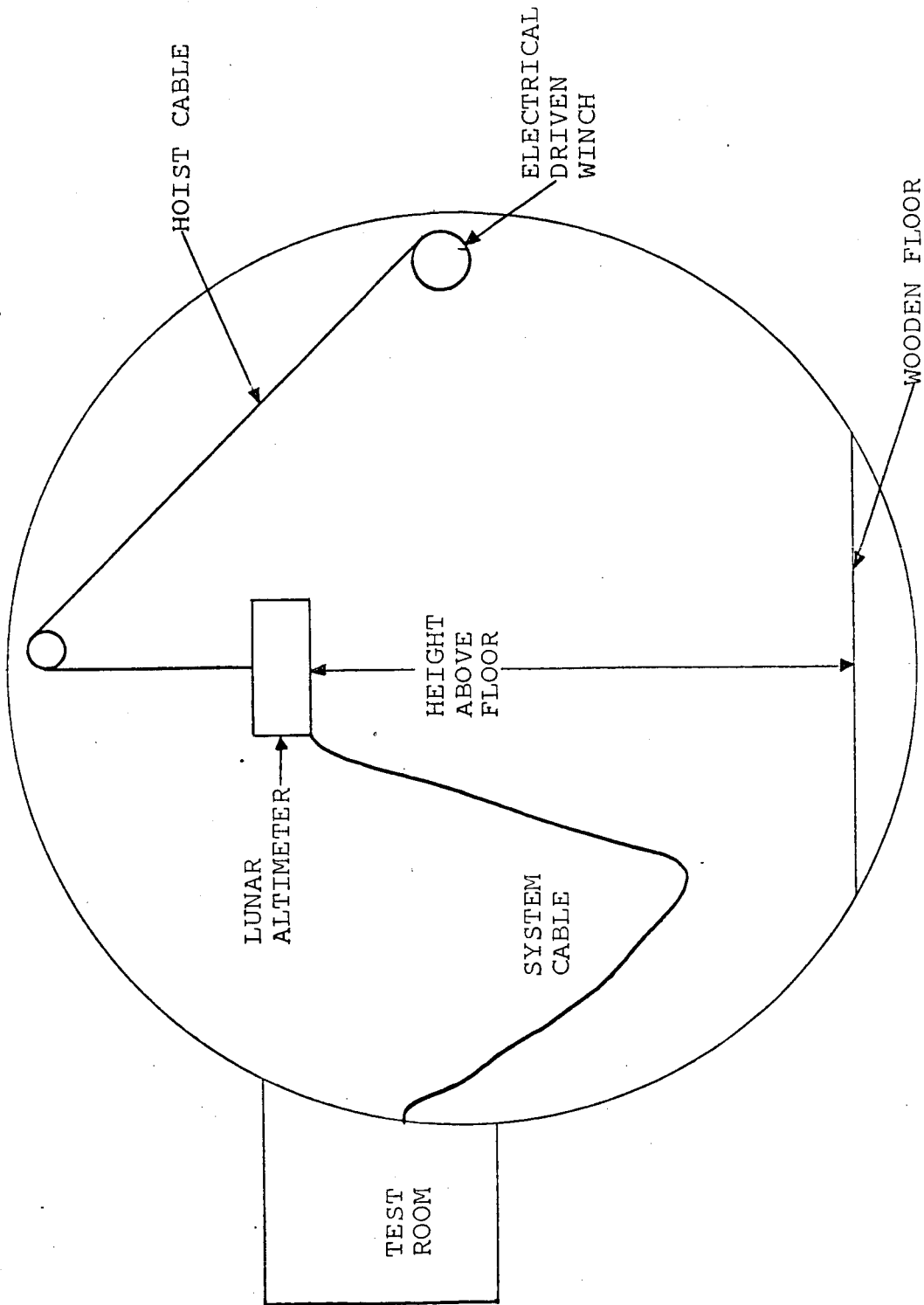A _____⌄_____⌄_____ B

|←———— T ————→|

FIGURE 7.0-1

ALTITUDE CHAMBER TEST SETUP

The second test was attempted on 22 January and 23 January, 1968. At this time, the x-ray tube was determined to have failed. Excessively large grid leakage current, in order of 0.5 milliamperes was noted. Since this condition results in improper pulse operation of the x-ray tube, the testing was regretfully terminated.

.8.0 PERSONNEL SAFETY

The NLRTS has two areas which can be a hazard to personnel, unless adequate safety design is included in the system. These are high voltage and x-ray radiation.

8.1 High Voltage

The x-ray Source Subsystem contains a power supply which delivers 100,000 volts to the x-ray tube. This high voltage supply is completely contained within an aluminum container. Thus the electrical field is confined to the inside of this grounded container and no high voltage hazard exists on the outside. The external power to operate the power supply is 28 volt DC.

8.2 Radiation Exposure

X-ray tube emits radiation only when a high potential and filament power is applied. The x-ray source will be turned on only during controlled ground test and during last phase of lunar landing. If required, the source can be shielded in the direction of the operating personnel during ground test. By using proper precautions, the radiation hazard is kept to a minimum.

On lunar landing, Figure 3.3-1 shows that on the average, 350 photons are received by the detector for each emitted pulse. At pulse repetition rate of 10^4 pulses per second, approximately 3.5×10^6 photons per second per 0.09 ft.^{2} will return with average energy at 45 keV. At the energies involved, 6×10^3 photons

8.2 Radiation Exposure (Continued)

per cm^2 per second are required to register 1 mr per hour.

The radiation level at lunar landing will be 4 mr per hour, compared to AEC's weekly suggested limit of 100 mr. The radiation level decreases with altitude, and total dose during landing should be far below 100 mr.

9.0 CONCLUSIONS AND RECOMMENDATIONS

9.1 Conclusion

Although functional test of the prototype system was not complet-
ed, preliminary tests and observations indicated that the system
would have successfully passed functional test. The x-ray sig-
nal reflected from ground and detected by the detector has more
than sufficient strength to operate the data processing electron-
ics. The data processing electronics have been calibrated and
bench tested using simulated signals.

The analysis of the system showed that the system is capable of
altitude measurement to 500 feet.

9.2 Recommendations

This section contains the modification and improvements to the
system which should be considered for any future program.

a) The x-ray tube should be replaced and functional test com-
   pleted to verify system parameters and errors.

b) The x-ray tube development should be concentrated in ob-
   taining higher peak power rating. An increase in the peak
   power will allow greater probability of communication
   per pulse at high altitude.

c) The prototype model used x-ray tube with a flat anode,
   which gives 360 degree emission. The useful beam is only
   about 30 degrees, resulting in 8% efficiency in use of x-
   ray output. An anode construction which gives a collima-
   ted beam is practical and should be considered. In addi-
   tion, the prototype source required construction as shown
   in Figure 4.1-3. A slanted anode x-ray tube will allow a
   more conventional packaging of the source, resulting in
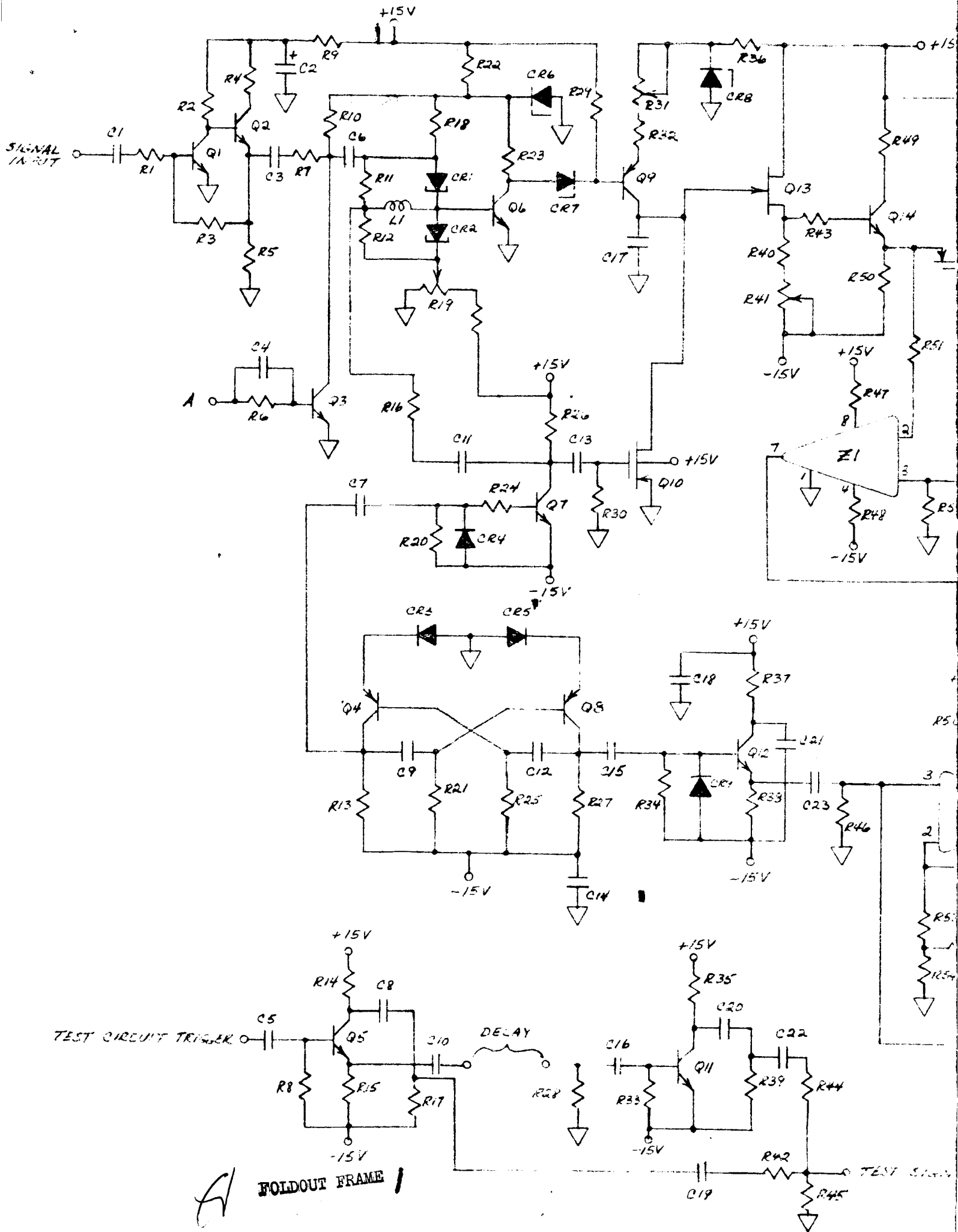   smaller source package.

9.2 Recommendations (Continued)

d) The high voltage supply was packaged using the maximum space available for it. The same supply has been packaged in space of 0.13 cu. ft. compared to 0.2 cu. ft. for the feasibility model. Reduction in source subsystem size from 0.55 cu. ft. to 0.28 cu. ft. should be possible.

e) In the feasibility model, the photomultiplier tube selected was an Amperex 56AVP-3, which is a high gain low noise tube. A smaller tube with ruggedized construction should be produced for a flight hardware.
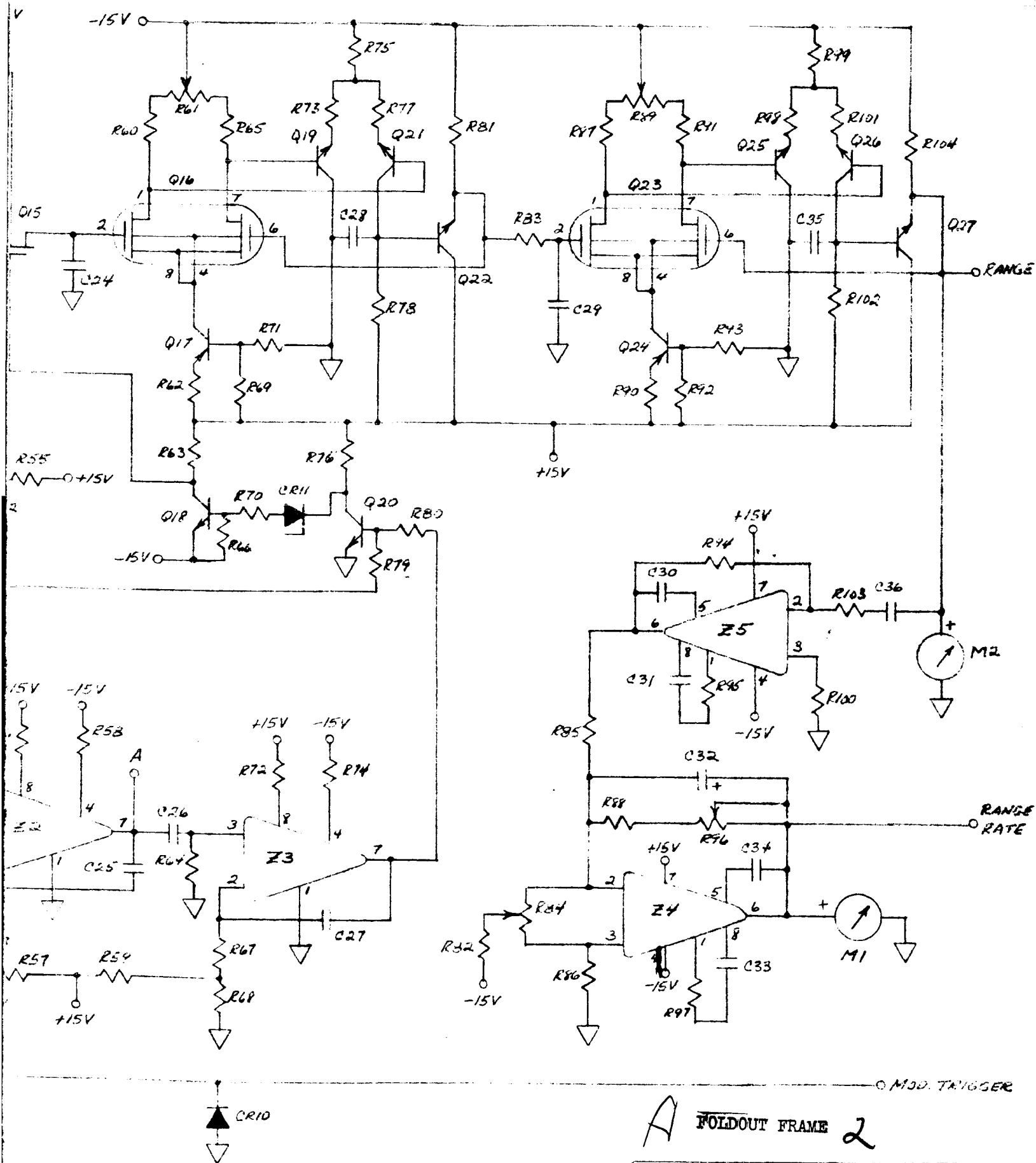
9.3 Additional Uses of X-Ray System

The principle used in pulse x-ray system for lunar altimeter is easily adaptable to several other uses. Some of these are discussed below.

a) Low Level Altimeter: The system can be used in tactical type altimeter applications. The system range, due to large attenuation by atmosphere, is limited to approximately 200 feet. The limited range of radiation will make the system useful in applications where secure altimeter is required, such as helicopters or low flying aircraft. Because of high accuracy at low altitudes, the altimeter would be very useful in landing and takeoff in low visibility conditions.

c) Air Density Measurement: The amount of x-ray signal backscattered into the detector by the atmosphere is directly proportional to the air density. Thus by measuring the relation between x-ray signal emitted and the backscatter signal detected, a measure of air density is available.

APPENDIX A

SCHEMATICS

SIGNAL INPUT

+15V

TEST CIRCUIT TRIGGER

DECAY

TEST SIGNAL

FOLDOUT FRAME 1

Z1

+15V -15V

A

R1 R2 R3 R4 R5 R6 R7 R8 R9 R10 R11 R12 R13 R14 R15 R16 R17 R18 R19 R20 R21 R22 R23 R24 R25 R27 R28 R30 R31 R32 R33 R34 R35 R36 R37 R39 R40 R41 R42 R43 R44 R45 R46 R47 R48 R49 R50 R51

C1 C2 C3 C4 C5 C6 C7 C8 C9 C11 C12 C13 C14 C15 C16 C17 C18 C19 C20 C21 C22 C23

Q1 Q2 Q3 Q4 Q5 Q6 Q7 Q8 Q9 Q10 Q11 Q12 Q13 Q14

CR1 CR2 CR3 CR4 CR5 CR6 CR7 CR8

L1

NLRTS
RANGE CIRCUIT

FOLDOUT FRAME 2

ELECTRONICS PARTS LIST

NLRTS RANGE CIRCUIT

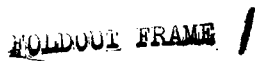| SYMBOL	PART NUMBER	DESCRIPTION	QTY. REQ'D.
C1, C13, 14, 18, 24		Capacitor, .01 μf	5
C2, C9		Capacitor, 1 μf	2
C3		Capacitor, .1 μf	1
C4		Capacitor, 75 pf	1
C5, 16, 25, 26		Capacitor, 100 pf	4
C6, 11		Capacitor, 10 pf	2
C7, 15, 17, 23		Capacitor, .001 μf	4
C8, 20, 21		Capacitor, 68 pf	3
C9, 12		Capacitor, 390 pf	2
C10		Capacitor, 470 pf	1
C19, 22		Capacitor, 150 pf	2
C27		Capacitor, .0015 μf	1
C28, 35		Capacitor, .002 μf	2
C30, 34		Capacitor, 200 pf	2
C31, 33		Capacitor, .005 μf	2
C32		Capacitor, 160 μf, NP	1
C36		Capacitor, 1 μf	1
CR1, 2	1N3717	Tunnel Diode	2
CR3, 4, 5, 9, 10	1N3605	Diode	5
CR6	1N825A	Zener Diode 6.2V	1
CR7	1N755A	Zener Diode 7.5V	1
CR8	1N759A	Zener Diode 12V	1
CR11	1N968B	Zener Diode 20V	1
L1		Inductor, 1 μH	1
M1, 2		DC Voltmeter, 0-5V 1K Ω/V	2

ELECTRONICS PARTS LIST

NLRTS RANGE CIRCUIT

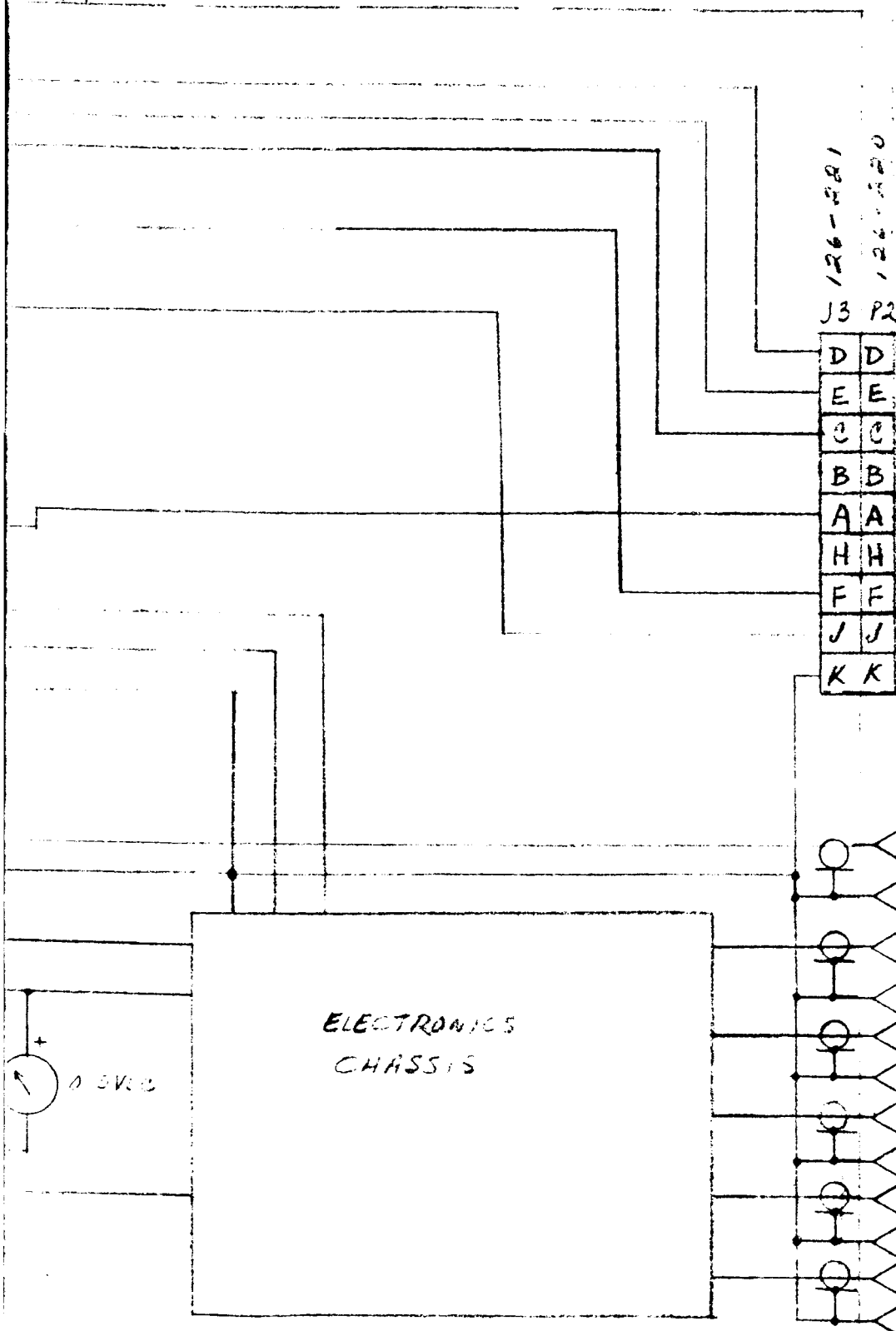| SYMBOL	PART NUMBER	DESCRIPTION	QTY. REQ'D.
Q1, 5, 6, 11, 12	FT709	Transistor	5
Q2	2N708	Transistor	1
Q3	2N2369	Transistor	1
Q4, 8	2N3906	Transistor	2
Q7, 14, 18, 20	2N3904	Transistor	4
Q9	2N995	Transistor	1
Q10, 15	FI100	Mosfet	2
Q13	FN490	FET	1
Q16, 23	2N3609	Dual Mosfet	2
Q17, 24	2N3504	Transistor	2
Q19, 21, 22, 25, 27	GME 4002	Transistor	6
R1, 4, 11, 12, 43, 49, 73, 77, 98, 101	RC07GF101J	Resistor, 100 Ω	10
R2, 16, 42, 44, 48 58, 74	RC07GF202J	Resistor, 2K	7
R3, 8, 24, 33, 34, 54, 66, 85, 86, 103	RC07GF102J	Resistor, 1K	10
R5	RC07GF201J	Resistor, 200 Ω	1
R6, 51, 79, 80	RC07GF302J	Resistor, 3K	4
R7	RC07GF221J	Resistor, 220 Ω	1
R9	RC07GF331J	Resistor, 330 Ω	1
R10, 20, 26, 46, 53, 55, 62, 64, 67, 69, 90, 92	RC07GF103J	Resistor, 10K	13
R13, 27, 70, 95, 97	RC07GF152J	Resistor, 1.5K	5
R14, 21, 25, 30, 35 37, 94, 100	RC07GF104J	Resistor, 100K	8
R15	RC07GF100J	Resistor, 10 Ω	1

NOTE: Unless otherwise noted, all Resistors are 1/4W, ± 5%

ELECTRONICS PARTS LIST

NLRTS RANGE CIRCUIT

SYMBOL	PART NUMBER	DESCRIPTION	QTY. REQ'D.
R17, 28, 38, 39, 45	RC07GF510J	Resistor, 51Ω	5
R18	RC07GF112J	Resistor, 1.1K	1
R19		Potentiometer, 100Ω	1
R22	RC07GF391J	Resistor, 390Ω	1
R23, 32	RC07GF561J	Resistor, 560Ω	2
R29	RC07GF362J	Resistor, 3.6K	1
R31		Potentiometer, 500Ω	1
R36	RC07GF301J	Resistor, 300Ω	1
R40, 50, 52, 76, 104,	RC07GF512J	Resistor, 5.1K	5
R47, 56, 68, 72	RC07GF511J	Resistor, 510Ω	4
R57, 59	RC07GF123J	Resistor, 12K	2
R60, 65, 87, 91	RN60D7502F	Resistor, 75K, 1%	4
R61, 89		Potentiometer, 50K	2
R71, 93	RC07GF513J	Resistor, 51K	2
R75, 99	RC07GF243J	Resistor, 24K	2
R78, 102	RC07GF753J	Resistor, 75K	2
R81	RC07GF153J	Resistor, 15K	1
R82	RC07GF155J	Resistor, 1.5M	1
R83	RC07GF514J	Resistor, 510K	1
R88	RC07GF752J	Resistor, 7.5K	1
R96		Potentiometer, 5K	1
R41, 84		Potentiometer, 20K	2
Z1, 2, 3	μA710C	Integrated Circuit	3
Z4, 5	μA709C	Integrated Circuit	2

NOTE: Unless otherwise noted, all Resistors are 1/4W, ± 5%

P1	J1
A	A
B	B
C	C
D	D
E	E
F	F
H	H
J	J
K	K

RV INPUT {

+

−

GROUND

RANGE

RANGE GATE

MODULATOR
SUPPLY
1000 V

510K

X-RAY TUBE
BIAS
SUPPLY
300 V

200K

ELECTRONICS
SUPPLY
±15 V.   COM

PM TUBE
HIGH VOLTAGE
SUPPLY
2000 V

SIGNAL OUTPUT
J6-625B/J

RAY

J3 P2

D	D	} -28V TO SOURCE SUBSYSTEM
E	E	+
C	C	X-RAY TUBE FILAMENT P.S. (+)
B	B	
A	A	X-RAY TUBE BIAS
H	H	
F	F	X-RAY TUBE FILAMENT P.S. (-)
J	J	MODULATOR H.V.
K	K	GROUND

ELECTRONICS
CHASSIS

-2KV TO FM TUBE
J4 UG-931/U

MODULATOR TRIGGER
J5 UG-625B/U

TEST TRIGGER INPUT
J6 UG-625B/U

} TEST SIGNAL DELAY
J7-J8 UG-625B/U

TEST SIGNAL OUTPUT
J9 UG-625B/U

NERTS
DATA PROCESSING
SUB-SYSTEM

APPENDIX B

CALIBRATION PROCEDURE

RANGE CIRCUIT CALIBRATION

1. Using coaxial cables, connect MOD TRIGGER to TEST IN and TEST OUT to SIGNAL INPUT.

2. Apply 28 volt DC to data processing electronics and turn on DETECTOR POWER switch.

3. Ground pin 2 of second range follower (Q23). Adjust off-set pot (R89) for zero reading on RANGE meter. Remove ground from second follower input.

4. Ground pin 2 of first range follower (Q16). Adjust off-set pot (R61) for zero reading on RANGE meter. Remove ground from first follower input.

5. Observe the waveform at emitter of current source (Q9). Adjust flip-flop trigger pot (R19) for a symmetrical square wave.

6. Observe the waveform across time base capacitor (C17). Adjust range slope pot (R31) so that the voltage rise slope is 5 volts per 1 microsecond.

7. Connect a 50 ohm delay line or cable between the DELAY connectors. The delay is to be selected for desired range.

8. Select two 50 ohm delay lines, one 40 nanoseconds and other 1 microsecond.

9. Connect short delay line between DELAY connectors. Adjust range zero pot (R41) for 10 feet indication on RANGE meter.

10. Connect long delay line between DELAY connectors. Adjust range slope pot (R31) for 500 feet indication on RANGE meter.

11. Repeat Steps 9 and 10 until no further adjustment is required.